*Chem. Soc. Rev.*, 1989, **18**, 285–316

# Heterogeneous Redox Catalysts for Oxygen and Chlorine Evolution

By Andrew Mills
DEPARTMENT OF CHEMISTRY, UNIVERSITY COLLEGE OF SWANSEA, SINGLETON PARK, SWANSEA, SA2 8PP

## 1 Introduction

The general redox reaction

$$n_2Ox_1 + n_1Red_2 \longrightarrow n_2Red_1 + n_1Ox_2 \quad (1)$$

comprising the two redox couples

$$Ox_1 + n_1e^- \rightleftharpoons Red_1 \quad (2)$$

and

$$Red_2 \rightleftharpoons Ox_2 + n_2e^- \quad (3)$$

is thermodynamically feasible, provided

$$\Delta E = E_1 - E_2 > 0\ V \quad (4)$$

where $E_1$ and $E_2$ are the equilibrium reduction potentials of redox couples 1 and 2, respectively. However, there exist many such feasible redox reactions which do not proceed at a measurable rate owing to their high activation energy barriers. An excellent example of this is provided by solutions of ceric sulphate, or potassium permanganate, made up in $H_2SO_4$ (typically 0.5 mol $dm^{-3}$), which are common in most laboratories and often used in redox titrations. These solutions are extremely stable and can last for years, however, in terms of thermodynamics they are unstable, since both oxidants have redox potentials greater than that of the $O_2/H_2O$ couple and, therefore, are capable of oxidizing water to $O_2$. For both $Ce^{IV}$ and $MnO_4^-$ ions the high kinetic stability of their solutions is due to a large activation energy barrier which in turn arises because the homogeneous oxidation of water requires four consecutive electron transfer steps involving the reactive and high energy species, $OH^{\bullet}$, $H_2O_2$, and $O_2^{\bullet}$ as intermediates.

A system in which two or more redox couples are present together but are not in equilibrium, *i.e.* $\Delta E \neq 0$ V, is often called a 'polyelectrode'.[1] A redox catalyst is a substance which is able to lower the activation barrier associated with a kinetically stable polyelectrode, such as the $Ce^{IV}/H_2O$ system and, in so doing, increases the rate of electron transfer to a measurable value. Although it is

[1] M. Spiro, *Chem. Soc. Rev.*, 1986, **15**, 141.

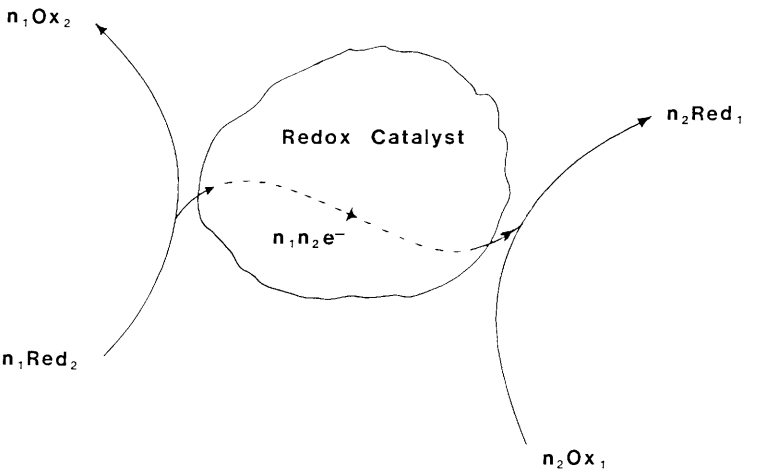


**Figure 1** *Schematic illustration of the usual role of a heterogeneous redox catalyst as an electron conductor in mediating the general reaction:*

$$n_2Ox_1 + n_1Red_2 \longrightarrow n_2Red_1 + n_1Ox_2$$

possible to have both homogeneous and heterogeneous redox catalysts for a particular reaction, it is examples of the latter which dominate the literature. The work of Spiro and his collaborators in this area of heterogeneous redox catalysis has advanced the subject significantly.[1] In particular, through an examination of over 70 different redox systems, they have demonstrated that the role of the redox catalyst is often simply that of a conductor of electrons,[2] as illustrated in Figure 1 for the general redox reaction 1. From this electrochemical approach to redox catalysis, the kinetics of catalysis of reaction 1 can be predicted from the current–voltage curves of the two contributing couples, *i.e.* reactions 2 and 3, and the appropriate electrochemical equations, *provided* the two couples act independently of one another. This assumption is often referred to as the Wagner–Traud additivity principle after its early exponents[3] and has been extensively and positively tested for over the years, with the discovery of few exceptions.[1,2]

It is appropriate at this point to introduce the concept of electrochemical reversibility. For a given electrode the more electrochemically reversible a couple is the faster the exchange of electrons between its oxidized and reduced forms occurs at the electrode. A measure of this electron exchange rate is provided by the exchange current density, $i_0$ and, typically,[2] for a reversible reaction $i_0$ is $\geqslant 10^{-6}$ A cm$^{-2}$, and for an irreversible reaction $i_0$ is $\leqslant 10^{-10}$ A cm$^{-2}$. From the electrochemical model and the concept of electrochemical reversibility it is possible to identify three different cases for the redox catalysis of reaction 1, and these are described in Table 1.

[2] M. Spiro and A. B. Ravnö, *J. Chem. Soc.*, 1965, 78.
[3] C. Wagner and W. Traud, *Z. Elektrochem.*, 1938, **44**, 391.

**Table 1** *Three cases for redox catalysis for the reaction*

$$n_2Ox_1 + n_1Red_2 \longrightarrow n_2Red_1 + n_1Ox_2$$

| *Case* | $Ox_1/Red_1$ | $Ox_2/Red_2$ | *Marked Catalysis?* | *Comments* |
|---|---|---|---|---|
| (1) | Rev. | Rev. | V. likely | However, it is also likely that the reaction will proceed at a measurable rate in the absence of a redox catalyst and this homogeneous reaction may obscure the redox catalytic effect. |
| (2) (a) | Rev. | Irrev. | Possible | This combination will often lead to the most spectacular examples of catalysis, since the homogeneous reaction is unlikely to occur at a measurable rate. |
| (b) | Irrev. | Rev. | Possible | |
| (3) | Irrev. | Irrev. | V. unlikely | It is unlikely that either the homogeneous or heterogeneous reaction would occur at a measurable rate. |

## 2 Background History

As the title suggests this review is concerned with heterogeneous redox catalysts which are able to mediate the oxidation of water to $O_2$, or chloride to $Cl_2$, by oxidants with redox potentials ($E_1$) which satisfy equation 4, where $E_2$ is the the equilibrium potential of the $O_2/H_2O$ or $Cl_2/Cl^-$ redox couple, respectively. Interest in such materials has primarily arisen from work into photochemical systems capable of efficiently collecting and storing solar energy in the form of a chemical fuel, which gained its greatest impetus, in terms of funding, following the oil crisis of the mid-seventies.[4,5] A major approach in this area of research is the development of an artificial photosystem capable of splitting water into hydrogen and oxygen, *i.e.*

$$2H_2O \xrightarrow[\text{sunlight}]{\text{photochemical system}} 2H_2 + O_2 \qquad (5)$$

More recently this research [5] has extended to the development of photochemical systems capable of splitting HCl into hydrogen and chlorine, *i.e.*

$$2HCl \xrightarrow[\text{sunlight}]{\text{photochemical system}} H_2 + Cl_2 \qquad (6)$$

In both cases, with the absorption of a photon of light, the photochemical system should generate a strong oxidant, capable of oxidizing water to $O_2$ (or $Cl^-$ to $Cl_2$) and a strong reducing agent, capable of reducing water to $H_2$. Thus, essential to the efficient operation of any one of these photochemical systems is the incorporation of redox catalysts for water (or $Cl^-$) oxidation and water

[4] A. Mills, *Sci. Tech. Rev.* (*Univ. Wales*), 1988, **4**, 39.
[5] 'Energy Resources Through Photochemistry and Catalysis,' ed. M. Grätzel, Academic Press, New York, 1983.

**Table 2** *Heterogeneous oxygen catalysts*

| *Catalyst* | *Oxidant* | *Ref.* |
|---|---|---|
| Pt foil | $Ce^{IV}$ ions (2 mol $dm^{-3}$ $HClO_4$) | 2 |
| $RuO_2 \cdot xH_2O$ (powder) | $Ce^{IV}$ ions (0.5 mol $dm^{-3}$ $H_2SO_4$) | 7—20 |
| (colloid) | | 21—23 |
| $RuO_2 \cdot xH_2O$ (powder) | $Ru(bpy)_3^{3+}$ [a] (chemically generated) | 7,8,24,25 |
| (colloid) | | 26 |
| $RuO_2 \cdot xH_2O$ (powder) | $Ru(bpy)_3^{3+}$ (generated photochemically) | 24,25,27—32 |
| (colloid) | | 26,28,33 |
| $RuO_2 \cdot xH_2O$ (colloids and powders) | Other oxidants including: $Fe(bpy)_3^{3+}$, $Tl^{3+}$, $BrO_3^-$, $MnO_4^-$ | 15,28,34,35 |
| $RuO_2 \cdot xH_2O$ on various supports including: $TiO_2$, $Al_2O_3$, clay, and zeolite | $Ce^{IV}$ ions, $Ru(bpy)_3^{2+}$, and other oxidants | 12,20,22,25, 29,31,36—40 |
| $PtO_2$ (Adams) | $Ce^{IV}$ ions (0.5 mol $dm^{-3}$ $H_2SO_4$) | 15,41 |
| $IrO_2$ | as above | 15,25,26,40 |
| $IrO_2 \cdot xH_2O$ | as above | 42 |
| $MnO_2$ | $Ru(bpy)_3^{3+}$ | 23,25,29,43 |
| $Rh_2O_3$ | as above | 25,29 |
| Prussian blue | $Ce^{IV}$ ions and $Ru(bpy)_3^{3+}$ | 44—46 |
| $[(bpy)_2Mn^{III}(\mu\text{-}O)_2Mn^{IV}(bpy)_2](ClO_4)_3$ | $Ce^{IV}$ ions | 47,48 |
| $[(phen)_2Mn^{III}(\mu\text{-}O)_2Mn^{IV}(phen)_2](ClO_4)_3$ [b] | $Ce^{IV}$ ions | 47 |
| $[(NH_3)_4Ru(NH_2)Ru(NH_3)_4]Cl_4$ | $Ce^{IV}$ ions | 49 |
| *trans*-$Ru(bpy)_2(H_2O)_2^{2+}$ | $Ru(bpy)_3^{3+}$ | 50 |

[a] bpy = 2,2′-bipyridine. [b] phen = 1,10-phenanthroline

reduction. These catalysts should be stable, specific, and fast-acting towards their respective redox reactions.

As indicated above, most of the research in this area has been concerned with the photosplitting of water, *i.e.* reaction 5. A great deal of progress has been made in the area of redox catalysts for water reduction, *i.e.* $H_2$ catalysts, and there are now materials such as colloidal Pt which are able to act in the μs timescale.[6] In contrast, progress in the area of water oxidation catalysts ($O_2$ catalysts) has been slow, since most of the materials tested appear to be either inactive or themselves undergo anodic corrosion when subjected to the strong oxidizing conditions necessary to oxidize water to $O_2$. Table 2 provides a list of the different materials which have been reported as active $O_2$ catalysts and the oxidizing agents which have been used to test them.[7-50] In contrast to the

[6] A. Demortier, M. De. Backer, and G. Lepoute, *Nouv. J. Chim.*, 1983, **7**, 421 and references therein.
[7] J. Kiwi and M. Grätzel, *Chemia*, 1976, **33**, 289.
[8] J. Kiwi, *Isr. J. Chem.*, 1979, **18**, 369.

situation with $O_2$ catalysts, there have been relatively few reports of $Cl_2$ catalysts and in most cases $Ce^{IV}$ ions in 0.5 mol $dm^{-3}$ $H_2SO_4$ were used as the oxidant.[51,52]

The choice of oxidizing agent for testing a new material for possible $O_2$, or $Cl_2$, catalytic activity is important and Table 3 lists some which have been used for this purpose.[53] In Table 3 we have calculated for each oxidant the value of $\Delta E$ for the oxidation of $H_2O$ to $O_2$, $\Delta E(O_2)$, and $Cl^-$ to $Cl_2$, $\Delta E(Cl_2)$. An oxidant will be thermodynamically 'stable' to water (or $Cl^-$) if $\Delta E(O_2)$ [or $\Delta E(Cl_2)$] is $-$ve. Usually, under ambient conditions and in the presence of water alone (or with


[9] K. Kalyanasundaram and M. Grätzel, *Angew. Chem., Int. Ed. Engl.*, 1979, **18**, 701.
[10] J. Kiwi, M. Grätzel, and G. Blondeel, *J. Chem. Soc., Dalton Trans.*, 1983, 2215.
[11] A. Mills and M. L. Zeeman, *J. Chem. Soc., Chem. Commun.*, 1981, 948.
[12] A. Mills, *J. Chem. Soc., Dalton Trans.*, 1982, 1213.
[13] A. Mills, C Lawrence, and R. Enos, *J. Chem. Soc., Chem. Commun.*, 1984, 1436.
[14] A. Mills, S. Giddings, and I. Patel, *J. Chem. Soc., Faraday Trans. 1*, 1987, **83**, 2317.
[15] A. Mills, S. Giddings, I. Patel, and C. Lawrence, *J. Chem. Soc., Faraday Trans. 1*, 1987, **83**, 2331.
[16] A. Mills and S. Giddings, *Inorg. Chim. Acta*, 1989, **158**, 49.
[17] A. Mills, S. Giddings, N. McMurray, and G. Williams, *Inorg. Chim. Acta*, 1989, **159**, 7.
[18] A. Mills and N. McMurray, *J. Chem. Soc., Faraday Trans. 1*, accepted for publication.
[19] A. Mills and N. McMurray, *J. Chem. Soc., Faraday Trans. 1*, accepted for publication.
[20] G. Blondeel, A. Harriman, G. Porter, D. Urwin, and J. Kiwi, *J. Phys. Chem.*, 1983, **87**, 2629.
[21] A. Mills and N. McMurray, *J. Chem. Soc., Faraday Trans. 1*, 1988, **84**, 379.
[22] C. Minero, E. Lorenzi, E. Pramauro, and E. Pelizzetti, *Inorg. Chim. Acta*, 1984, **91**, 301.
[23] A. Harriman, M.-C. Richoux, P. A. Christensen, S. Mosseri, and P. Neta, *J. Chem. Soc., Faraday Trans. 1*, 1987, **83**, 3001.
[24] J.-P. Collin, J.-M. Lehn, and R. Zeissel, *Nouv. J. Chim.*, 1982, **6**, 405.
[25] J.-M. Lehn, J.-P. Sauvage, and R. Ziessel, *Nouv. J. Chim.*, 1979, **3**, 423.
[26] V. Ya. Shafirovich and V. V. Strelets, *Nouv. J. Chim.*, 1982, **6**, 183.
[27] A. Harriman, G. Porter, and P. Walters, *J. Chem. Soc., Faraday Trans. 2*, 1981, **77**, 2373.
[28] K. Kalyanasundaram, O. Mićić, E. Pramauro, and M. Grätzel, *Helv. Chim. Acta*, 1979, **62**, 2432.
[29] J.-M. Lehn, J. P. Sauvage, and R. Ziessel, *Nouv. J. Chim.*, 1980, **78**, 339.
[30] A. Juris and L. Moggi, *Int. J. Solar Energy*, 1983, **1**, 273.
[31] K. Kalyanasundaram and M. Grätzel, *Angew. Chem., Int. Ed. Engl.*, 1979, **18**, 701.
[32] M. Kaneko, N. Awaya, and A. Yamada, *Chem. Lett.*, 1982, **17**, 619.
[33] M. Neumann-Spallart, *J. Chem. Soc., Faraday Trans. 1*, 1985, **81**, 601.
[34] J. Kiwi, *J. Chem. Soc., Faraday Trans. 2*, 1982, **78**, 339.
[35] E. Pramauro and E. Pelizzetti, *Inorg. Chim. Acta*, 1980, **45**, L131.
[36] D. Duonghong, W. Erbs, L. Shuben, and M. Grätzel, *Chem. Phys. Lett.*, 1983, 266.
[37] H. Nijs, M. I. Cruz, J. J. Fripiat, and H. Van Damme, *Nouv. J. Chim.*, 1982, **6**, 551.
[38] D. H. M. W. Thewissen, M. Eeuwhort-Reinten, K. Timmer, A. H. A. Tinnemans, and A. Mackor, *J. R. Soc. Neth. Chem. Soc.*, 1982, **101/2**, 79.
[39] R. Humphry-Baker, J. Lilie, and M. Grätzel, *J. Am. Chem. Soc.*, 1982, **104**, 422.
[40] P. Baltzer, R. S. Davidson, A. C. Tseung, M. Grätzel, and J. Kiwi, *J. Am. Chem. Soc.*, 1984, **106**, 1504.
[41] J. Kiwi and M. Grätzel, *Angew. Chem., Int. Ed. Engl.*, 1978, **17**, 860.
[42] A. Harriman, J. M. Thomas, and G. R. Millward, *New J. Chem.*, 1987, **11**, 757.
[43] Y. Okuno, O. Yonemitsu, and Y. Chiba, *Chem. Lett.*, 1983, 815.
[44] P. A. Christensen, A. Harriman, P. Neta, and M.-C. Richoux, *J. Chem. Soc., Faraday Trans. 1*, 1985, **81**, 2461.
[45] M. Kaneko, N. Takabayshi, and A. Yamada, *Chem. Lett.*, 1982, 1647.
[46] M. Kaneko, N. Takabayshi, Y. Yamaguchi, and A. Yamada, *Bull. Chem. Soc. Jpn.*, 1984, **57**, 156.
[47] R. Ramaraj, A. Kira, and M. Kaneko, *Angew. Chem., Int. Ed. Engl.*, 1986, **25**, 825.
[48] R. Ramaraj, A. Kira, and M. Kaneko, *Chem. Lett.*, 1987, 261.
[49] R. Ramaraj, A. Kira, and M. Kaneko, *J. Chem. Soc., Chem. Commun.*, 1986, 1707.
[50] H. Hijs, M. Cruz, J. Fripiat, and H. Van Damme, *J. Chem. Soc., Chem. Commun.*, 1981, 1026.
[51] J. Kiwi and M. Grätzel, *Chem. Phys. Lett.*, 1981, **78**, 241.
[52] A. Mills and A. Cook, *J. Chem. Soc., Faraday Trans. 1*, 1988, **84**, 1691.
[53] R. C. Weast in 'CRC Handbook of Chemistry and Physics,' CRC Press, Boca Raton, Florida, 61st edn., 1980, D155.

**Table 3** *A list of oxidants and their $\Delta E$ values for $O_2$ or $Cl_2$ evolution*

| *Oxidant* | *Electrochemical Reversibility* † | *Standard Redox Potential*[53] (V *vs.* NHE) (*Initial* ⟶ *Final*) *Oxidation State* | $\Delta E(O_2)$ (V) | $\Delta E(Cl_2)$ (V) |
|---|---|---|---|---|
| $S_2O_8^{2-}$ | Irrev. | 2.01 (+7 ⟶ +6) | 0.78 | 0.65 |
| $Ce^{IV}$ ions (2 mol $dm^{-3}$ $HClO_4$) | | 1.70 (+4 ⟶ +3) | 0.47 | 0.34* |
| $MnO_4^-$ | Irrev. | 1.68 (+7 ⟶ +4) | 0.45 | 0.32* |
| $IO_4^-$ | Rev. | 1.65 (+7 ⟶ +5) | 0.42 | 0.29 |
| $PbO_2$ | — | 1.46 (+4 ⟶ +2) | 0.23 | 0.10* |
| $ClO_3^-$ | M. rev. | 1.45 (+5 ⟶ −1) | 0.22 | 0.09 |
| $Ce^{IV}$ ions (0.5 mol $dm^{-3}$ $H_2SO_4$) | Rev. | 1.45 (+4 ⟶ +3) | 0.22 | 0.09 |
| $Cl_2$ | M. rev. | 1.36 (0 ⟶ −1) | 0.13 | 0 |
| $BrO_3^-$ | Rev. | 1.44 (+5 ⟶ −1) | 0.21 | 0.08 |
| $Cr_2O_7^{2-}$ | Irrev. | 1.33 (+6 ⟶ +3) | 0.10 | −0.03 |
| $Ru(bpy)_3^{3+}$ | Rev. | 1.27 (+3 ⟶ +2) | 0.04 | −0.09 |
| $Tl^{3+}$ | Rev. | 1.25 (+3 ⟶ +1) | 0.02 | −0.11 |
| $MnO_2$ | — | 1.21 (+4 ⟶ +2) | −0.02 | −0.15* |
| $IO_3^-$ | M. rev. | 1.09 (+5 ⟶ −1) | −0.14 | −0.27 |
| $Fe(bpy)_3^{3+}$ | Rev. | 0.98 (+3 ⟶ +2) | −0.25 | −0.38 |

* Mixtures of the oxidant and $Cl^-$ are kinetically unstable. † On Pt electrodes (Rev. = reversible: Irrev. = irreversible; M. Rev. = moderately reversible)[2]

$Cl^-$ ions) such oxidants do not generate $O_2$ (or $Cl_2$) at a measurable rate and the introduction of a redox catalyst does not speed up the reaction. At pH 0 all the oxidants listed in Table 3 are stable in water and in brine, although in the latter there are a few notable exceptions such as $PbO_2$, $MnO_2$, and $Ce^{IV}$ ions (2 mol $dm^{-3}$ $HClO_4$).

In order to test a new material for $O_2$ or $Cl_2$ catalytic activity the oxidant must be stable, cheap, and simple (*i.e.* preferably involve the transfer of only one electron). In addition, from Table 1, it would appear that an appropriate oxidant must be electrochemically reversible at the redox catalyst. From Table 2 it is

**Table 4** *A comparison between* $Ce^{IV}$ *and* $Ru(bpy)_3^{3+}$ *as the 'test' oxidant for determining the* $O_2$ *catalytic activity of a new material*

| *Property* | $Ce^{IV}$ | $Ru(bpy)_3^{3+}$ | *Comments* |
|---|---|---|---|
| Redox potential[a] | 1.44 | 1.27 | $Ce^{IV}$ ions are able to oxidize water to $O_2$ and $Cl^-$ to $Cl_2$ whereas $Ru(bpy)_3^{3+}$ ions are only able to oxidize water to $O_2$. For $Ru(bpy)_3^{3+}$, at pH 0, the overpotential for the oxidation of water to $O_2$ is insufficient to drive the reaction. |
| Price | Cheap | Expensive | The ruthenium species is usually purchased or prepared in its stable $2^+$ form. |
| Preparation required | None | Some | Analytical volumetric solutions of $Ce^{IV}$ ions in $H_2SO_4$ may be readily purchased, whereas $Ru(bpy)_3^{3+}$ must be generated chemically or photochemically from its stable $2^+$ form. |
| Operational pH range | < pH 1 | pH 1—6 | $Ce^{IV}$ ions undergo hydrolysis at pHs > 1. In contrast solutions of $Ru(bpy)_3^{3+}$ are relatively stable ($t_{\frac{1}{2}}$ > 1.5 min)[30,54,55] up to pH 6. |
| Long-term stability | Excellent | Poor | In 0.5 mol $dm^{-3}$ $H_2SO_4$, solutions containing $Ce^{IV}$ ions can last years, whereas solutions containing $Ru(bpy)_3^{3+}$ ions will last only 1—2 weeks.[30,51,52] At higher pHs the stability of the $Ru(bpy)_3^{3+}$ solutions decreases markedly. |
| Photochemical generation | No | Yes | $Ru(bpy)_3^{3+}$ can be readily photogenerated using sacrificial electron acceptors such as $Co(NH_3)_5Cl^{2+}$ or $S_2O_8^{2-}$. This coupled with the interest in water splitting photochemical systems is largely responsible for the popularity of $Ru(bpy)_3^{3+}$ as a test oxidant. |

[a] In 0.5 mol $dm^{-3}$ $H_2SO_4$, *vs.* NHE.

clear that the most popular oxidants for testing $O_2$ catalytic activity are $Ce^{IV}$ and $Ru(bpy)_3^{3+}$ ions. This seems appropriate since they are both electrochemically reversible on a Pt electrode (see Table 3) and it seems probable that they would behave similarly on most conducting materials. A comparison between the two oxidants is provided in Table 4.[54,55] From Table 4 it is clear why $Ce^{IV}$ ions are the most commonly used oxidant for testing a new material for $O_2$ or $Cl_2$ activity. It is worth noting also the general finding[5] that any material identified as a good $O_2$ catalyst using $Ce^{IV}$ ions as the 'test' oxidant, appears also to be a good $O_2$ catalyst when used at higher pHs with, say, $Ru(bpy)_3^{3+}$. Typically, a $Ce^{IV}$ 'test' system comprises a solution of $Ce^{IV}$ ions ($3.6 \times 10^{-3}$ mol $dm^{-3}$) in 0.5 mol $dm^{-3}$ $H_2SO_4$ and a catalyst concentration of *ca.* 0.1 g $dm^{-3}$.

### 3 Ruthenium Dioxide Hydrate

**A. $O_2$ Catalysis.**—From Table 2 it is apparent that ruthenium dioxide hydrate is

[54] C. Creutz and N. Sutin, *Proc. Natl. Acad. Sci. U.S.A.*, 1975, **72**, 2858.
[55] P. K. Ghosh, B. S. Brunschwig, M. Chou, C. Creutz, and N. Sutin, *J. Am. Chem. Soc.*, 1984, **106**, 4772.

one of the most popular $O_2$ catalysts. However, extensive and detailed research has now established[11–15] that there are two important and very different types of this hydrate: the first we shall refer to as $RuO_2{\cdot}xH_2O$ and the second as $RuO_2{\cdot}yH_2O$*. $RuO_2{\cdot}xH_2O$ is highly hydrated (% $H_2O$ content $\geqslant$ 24%) and may be purchased from suppliers such as: Johnson Matthey, Aldrich, Strem, and Englehard or prepared *via* the alkaline hydrolysis of an aerated aqueous solution of $RuCl_3{\cdot}nH_2O$. This form of ruthenium dioxide hydrate is *not* a good $O_2$ catalyst.[11–14] Indeed, in the presence of an excess of $Ce^{IV}$ ions in 0.5 mol $dm^{-3}$ $H_2SO_4$ it is completely oxidized to $RuO_4$ with the concomitant generation of $O_2$. Equations describing these two simultaneous reactions were found to be as follows:[14]

$$4Ce^{IV} + RuO_2{\cdot}xH_2O + 2H_2O \longrightarrow 4Ce^{III} + RuO_4 + xH_2O + 4H^+ \qquad (7a)$$

and

$$4zCe^{IV} + 2zH_2O \longrightarrow 4zCe^{III} + 4zH^+ + zO_2 \qquad (7b)$$

where $z \simeq 0.26$.

In our study of the anodic corrosion of $RuO_2{\cdot}xH_2O$ by $Ce^{IV}$ ions, *i.e.* reaction 7, initially we believed that the source of the water oxidized in reaction 7b originated from the hydrate itself rather than the solvent. However, the results of a more recent study carried out by our group,[56] using $O^{18}$-labelled water in the solvent and mass spectrometry for gas analysis, indicate that the $O_2$ generated in reaction 7b originates from the solvent. In this latter work we were also able to confirm that the $RuO_4$ also generated in the corrosion of $RuO_2{\cdot}xH_2O$ gains two O atoms from the solvent, as indicated in equation 7a.

If the $RuO_2{\cdot}xH_2O$ sample is annealed above ambient temperature in air for 5 h and then tested for $O_2$ catalytic activity, it undergoes less corrosion and behaves more like an $O_2$ catalyst than untreated $RuO_2{\cdot}xH_2O$.[15] Figure 2 illustrates the measured % corrosion and % $O_2$ yields when samples of $RuO_2{\cdot}xH_2O$ which had been baked-out at different temperatures were injected into a $Ce^{IV}$ test solution. The % corrosion was determined from the amount of $RuO_4$ generated during the reaction and chemically trapped out as perruthenate using a solution of sodium hypochlorite incorporated in a flow system.[16] When measured in this way the highest % corrosion of ruthenium dioxide hydrate to $RuO_4$ was found to be *ca.* 86% and not 100% as might be expected. However, the % corrosion value of 86% represents a minimum estimate of the real value, since some of the $RuO_4$ generated reacted with the glassware and any exposed rubber tubing before reaching the chemical trap, as evidenced by the blackening of both. Other experiments with $RuO_4$ alone showed that the maximum collection efficiency of the hypochlorite trap flow system was 86% indicating that a recorded % corrosion value of 86% for a ruthernium(IV) oxide powder actually indicates 100% corrosion of the powder. The % $O_2$ yield was determined using an $O_2$ electrode incorporated at the end of the same flow system.[15]

[56] A. Mills, R. Mason, and D. Milton, *J. Less-Common Metals*, accepted for publication.

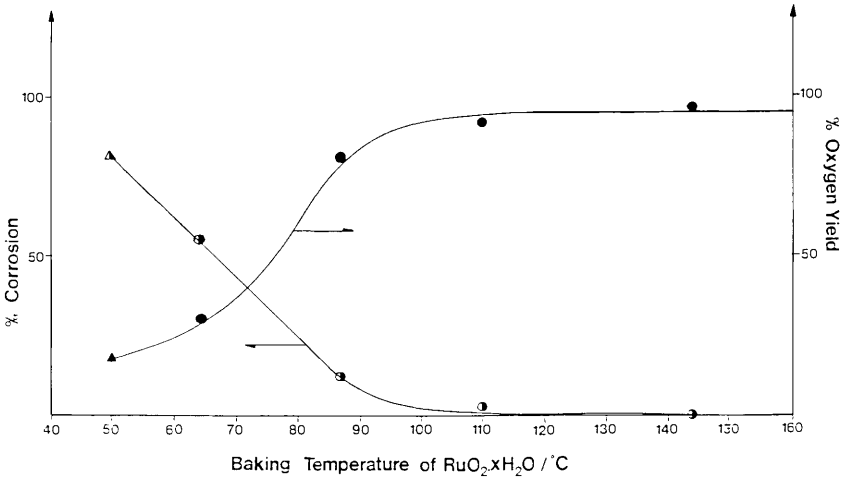


**Figure 2** *% $O_2$ yield (●) and % corrosion (○): observed on injecting samples* (7.5 mg *in* 7.5 $cm^{-3}$ *of* 0.5 mol $dm^{-3}$ $H_2SO_4$) *of* $RuO_2 \cdot xH_2O$, *baked-out at different temperatures for* 5 h, *into* 100 $cm^3$ *of a* $H_2SO_4$ *soluton* (0.5 mol $dm^{-3}$) *containing* $Ce^{IV}$ *ions* (3.6 × $10^{-3}$ mol $dm^{-3}$: ▲, ◭, *commercial* $RuO_2 \cdot xH_2O$ (*usually dried by the manufacturer at* 50 °C; ●, ○ *baked-out samples of* $RuO_2 \cdot xH_2O$ ($T$ = 298 K)

From the results illustrated in Figure 2 it is clear that samples of $RuO_2 \cdot xH_2O$ baked out at temperatures $\geqslant$144 °C are not only stable towards corrosion but also active as $O_2$ catalysts, *i.e.* they catalyse quantitatively the reaction

$$4Ce^{IV} + 2H_2O \longrightarrow 4Ce^{III} + 4H^+ + O_2 \qquad (8)$$

However, although samples of $RuO_2 \cdot xH_2O$ baked out at temperatures $\geqslant$144 °C are stable towards corrosion, it also appears that their $O_2$ catalytic activities decrease with increasing annealing temperature, as illustrated in Figure 3. Further work has estabished[15] that this drop in activity with increasing annealing temperature is primarily due to a decrease in specific surface area of the sample which, in turn, is due to the processes of sintering and crystallization. Indeed, anhydrous, highly crystalline $RuO_2$ appears inactive as a catalyst,[12,15] due to its very low specific surface area, typically $\leqslant 5$ $m^2$ $gm^{-1}$.

From the above work it appears that the optimum form of thermally activated ruthenium dioxide hydrate for $O_2$ catalysis is a sample of $RuO_2 \cdot xH_2O$ baked out at *ca.* 144 °C for 5 h in air. Throughout this paper we shall refer to this particular catalyst as $RuO_2 \cdot yH_2O$*. *To date this material appears to be the most active, stable heterogeneous* $O_2$ *catalyst developed.* Table 5 provides a list of oxidants which are able to oxidize water in the presence of $RuO_2 \cdot yH_2O$* and the observed $O_2$ yields. Thermal activation of $RuO_2 \cdot xH_2O$ to $RuO_2 \cdot yH_2O$* appears to be independent of the atmosphere under which the samples are annealed, *i.e.* an annealing environment of $N_2$ or $O_2$ does appear not to effect the $O_2$ catalytic activity or corrodibility of the final, activated sample of ruthenium dioxide

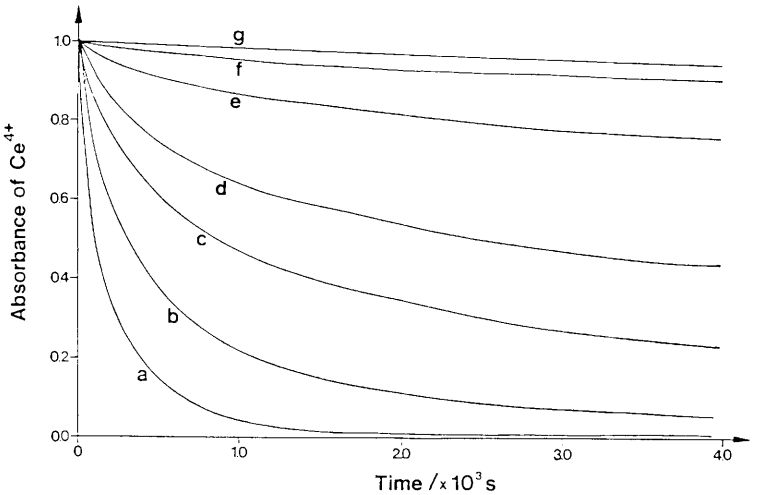


**Figure 3** *Absorbance* vs. *time plots, recorded using a* 1 cm *cell* ($\lambda$ = 430 nm), *showing the decay of* $Ce^{IV}$ *ions* (ca. 3.5 × $10^{-3}$ mol $dm^{-3}$) *after injection* (*at* $t$ = 0) *of* 90 $mm^3$ *of* 0.1 mol $dm^{-3}$ $Ce^{IV}$ *soluton into stirred dispersions of* ca. 175 μg *of* $RuO_2 \cdot xH_2O$ *in* 2.5 $cm^3$ *of* 0.5 mol $dm^{-3}$ $H_2SO_4$, *baked-out at different temperatures. The baking temperatures of the* $RuO_2 \cdot xH_2O$ *samples were:* (*a*) 140, (*b*) 250, (*c*) 400, (*d*) 550, (*e*) 700, (*f*) 900 °C *and* (*g*) *no sample* ($T$ = 298 K)

**Table 5** % $O_2$ *yield for a variety of oxidizing agents using* $RuO_2 \cdot yH_2O$* *as the redox catalyst* ($T$ = 298 K)

| *Oxidizing Agent* | *Initial* ⟶ *Final Oxidation State* | % $O_2$ *Yield* | *Comments* |
|---|---|---|---|
| $Ce^{IV}$ (0.5 mol $dm^{-3}$ $H_2SO_4$) | +4 ⟶ +3 | 97—102 | A rapid reaction, over in less than 10 min |
| $MnO_4^-$ | +7 ⟶ +4 | 99 | As for $Ce^{IV}$ |
| $IO_4^-$ | +7 ⟶ +5 | 104 | As for $Ce^{IV}$ |
| $BrO_3^-$ | +5 ⟶ −1 | 84 | A much slower reaction, complete after *ca.* 17 h |
| $PbO_2$ | +4 ⟶ +2 | 44 | A very slow and incomplete reaction |
| $MnO_2$ | +4 ⟶ +2 | 53 | As for $PbO_2$ |
| $ClO_3^-$ | +5 ⟶ −1 | 3 | Very little, if any, reaction |
| $Cr_2O_7^-$ | +6 ⟶ +3 | 0 | As for $ClO_3^-$ |
| $Ru(bpy)_3^{3+}$ | +3 ⟶ +2 | 0 | As for $ClO_3^-$ |
| $Ce^{IV}/Ce^{III}$ (1:10) (0.5 mol $dm^{-3}$ $H_2SO_4$) | +4 ⟶ +3 | 92 | A very slow reaction, complete after *ca.* 30 h |

hydrate. As you might expect, in contrast to $RuO_2 \cdot xH_2O$, $RuO_2 \cdot yH_2O$* is much less hydrated (% $H_2O$ content ⩽ 12%). The relationship between the % $H_2O$ content of a sample of ruthenium dioxide hydrate and its corrodibility, as measured by a $Ce^{IV}$ test system, is illustrated in Figure 4.

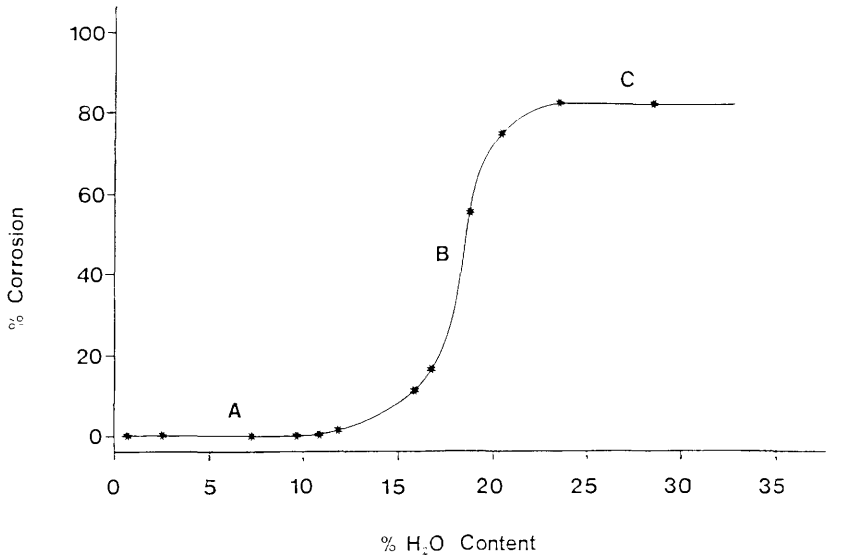


**Figure 4** *% Corrosion* vs. % $H_2O$ *content for samples of highly hydrated* $RuO_2 \cdot xH_2O$, *not heat-treated and heat-treated at different temperatures over the range* 60—400 °C. *The samples can be divided into three distinct classes: (A) non-corrodible;* % $H_2O$ *content* $\leqslant$ 10%, *(B) only partly corrodible, with the* % *corrosion increasing with increasing* % $H_2O$ *content;* 24% > % $H_2O$ *content* > 10% *and (C) completely corrodible;* % $H_2O$ *content* $\geqslant$ 24% ($T$ = 298 K)

Interestingly, samples of ruthenium dioxide hydrate from Alfa and Fluka have been found not to be fully hydrated and typically possess a % $H_2O$ content of *ca.* 18%. These materials exhibit a much greater resistance towards corrosion (% corrosion 8—9%) and a high catalytic activity ($O_2$ yield = 92%). This discrepancy between different commercial samples of ruthenium dioxide hydrate may even extend to different batches from the same supplier and is almost certainly the cause for the marked discrepancies in $O_2$ catalytic activity reported for ruthenium dioxide hydrate over the years.[7-15] As might be expected, such anomalous samples of $RuO_2 \cdot xH_2O$ are readily converted into $RuO_2 \cdot yH_2O$* by annealing in air for 5 h at 144 °C.

It appears likely that anodic corrosion of any sample of ruthenium dioxide hydrate occurs at kink or other surface-defect sites and that such sites would be associated with a greater number of co-ordinated hydroxyl groups than at other surface sites. If this were the case it would help rationalize why the % $H_2O$ content of a sample of ruthenium dioxide hydrate provides some measure of its corrodibility (see Figure 4). By analogy with samples of hydrated $TiO_2$ it appears likely that heat treatment of $RuO_2 \cdot xH_2O$ brings about the loss of water from the samples *via* a 'condensation' reaction between the two hydroxyl groups on adjacent Ru surface atoms with the formation of a Ru–O–Ru bond.[56,57] This

[57] M. Primet, P. Pichat, and M.-V. Mathieu, *J. Phys. Chem.*, 1971, **75**, 1261.

process would lead to a less defective surface which might be expected to be less prone to corrosion.

**B. $Cl_2$ Catalysis.**—A convenient test system for a possible $Cl_2$ catalyst is provided by a $H_2SO_4$ solution (0.5 mol $dm^{-3}$) containing $Ce^{IV}$ and chloride ions. As indicated in Table 3, this system is thermodynamically unstable, $\Delta E > 0$ V, but, in practice, it is found to be kinetically stable. A 'good' $Cl_2$ catalyst would mediate the oxidation of the $Cl^-$ ions to $Cl_2$ by the $Ce^{IV}$ ions, *i.e.*

$$2Ce^{IV} + 2Cl^- \longrightarrow 2Ce^{III} + Cl_2 \qquad (9)$$

This test system was first suggested in 1981 by Kiwi and Grätzel[51] who also reported that $RuO_2 \cdot xH_2O$, supplied by Alfa, was able to catalyse reaction 9 as well as reaction 8 when chloride ions were added. In a typical experiment, the concentration of $Ce^{IV}$ ions and catalyst were $10^{-3}$ mol $dm^{-3}$ and $2 \times 10^{-3}$ mol $dm^{-3}$ (*ca.* 0.34 g $dm^{-3}$), respectively. At a $Cl^-$ concentration of $10^{-3}$ mol $dm^{-3}$ the reaction appeared to be 6% efficient and this could be increased to *ca.* 17% by increasing the $Cl^-$ concentration to 1 mol $dm^{-3}$. The low efficiency of $Cl_2$ evolution, observed even at high $Cl^-$ concentrations was attributed to competition between reactions 8 and 9.

Initially, it seems unlikely that $RuO_2 \cdot xH_2O$ would be able to mediate reaction 9 as claimed by Kiwi and Grätzel. However, with hindsight, this is not so unreasonable since the $RuO_2 \cdot xH_2O$ sample used by these workers was supplied by Alfa and therefore was quite likely partially dehydrated. As noted previously, such anomalous forms of $RuO_2 \cdot xH_2O$ are known to exhibit some $O_2$ catalyst activity and to have some stability against anodic corrosion.[15] Interestingly, if some $RuO_4$ were generated *via* reaction 7 it would be expected[58] to react with the $Cl^-$ ions present, particularly if the $Cl^-$ concentration was high, to form a mixture of water soluble ruthenium(IV) oxochlorides[58] and, presumably, $Cl_2$. If highly hydrated $RuO_2 \cdot xH_2O$ was used as the '$Cl_2$ catalyst' in his system then $RuO_4$ may not only be generated *via* reaction 7, but also *via* reaction 10.

$$RuO_2 \cdot xH_2O + 2H_2O + 2Cl_2 \longrightarrow RuO_4 + 4H^+ + 4Cl^- + xH_2O \qquad (10)$$

Indeed, the use of chlorine water to generate $RuO_4$ from $RuO_2 \cdot xH_2O$ is a well established procedure.[58]

Thermally activated ruthenium dioxide hydrate ($RuO_2 \cdot yH_2O$*) is not corroded readily by $Cl_2$ and we have established that it is able to mediate reaction 9 with 98% efficiency at $Cl^-$ concentrations $>0.2$ mol $dm^{-3}$. On reducing the $Cl^-$ concentration below this 'threshold' value the $Cl_2$ and $O_2$ yields decrease (98 to 0%) and increase (0 to 95%), respectively, as illustrated in Figure 5. These trends

[58] E. A. Seddon and K. R. Seddon, 'The Chemistry of Ruthenium,' Elsevier, Amsterdam, 1984, Chapters 3 and 5.

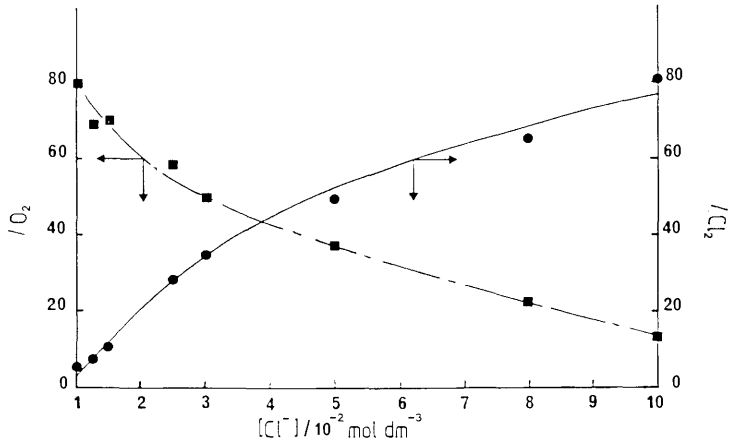


**Figure 5** *% $O_2$ and % $Cl_2$ yields, produced via reactions 8 and 9, determined as a function of $Cl^-$ concentration. These results were obtained by injecting 5 × $10^{-4}$ mol of $Ce^{IV}$ ions into 100 $cm^3$ $H_2SO_4$ solution (0.5 mol $dm^{-3}$) containing 10 mg of $RuO_2 \cdot yH_2O$* and a variety of different $Cl^-$ ion concentrations. Any $Cl_2$ generated was swept out by a continuously flowing $N_2$ stream and subsequently determined using a 'tri-iodide trap' ($T$ = 298 K)*

**Table 6** *% $O_2$ and % $Cl_2$ yields for a variety of different materials tested for $O_2$ and $Cl_2$ catalytic activity*[a]

| *Material* | *% $O_2$ Yield* | *% $Cl_2$ Yield* |
|---|---|---|
| $RuO_2 \cdot yH_2O$* | 97—102 | 98 |
| $RuO_2 \cdot xH_2O$ | 6 | 90 |
| $IrO_2$ | 0 | 81 |
| $PtO_2$ (Adams) | 0 | 68 |
| Pt | 0 | 64 |
| Au | 0 | 0 |
| $TiO_2$ | 0 | 0 |
| $SiO_2$ | 0 | 0 |

[a] Determined using 10 mg of redox catalyst in a $H_2SO_4$ solution containing $Ce^{IV}$ ions (100 $cm^3$; 3.6 × $10^{-3}$ mol $dm^{-3}$) and (for % $Cl_2$ yields only) $Cl^-$ ions (1 mol $dm^{-3}$); $T$ = 298 K.

in % $Cl_2$ and % $O_2$ as a function of [$Cl^-$] arise because reactions 8 and 9 are competitive and, as we shall see, the kinetics of reaction 9 are a function of the $Cl^-$ concentration.

Using a test system comprising $Ce^{IV}$ ions (100 $cm^3$, 3.6 × $10^{-3}$ mol $dm^{-3}$) in 0.5 mol $dm^{-3}$ $H_2SO_4$ and $Cl^-$ ions (1 mol $dm^{-3}$), 10 mg samples of a variety of different materials were tested for catalytic activity. The results of this work are summarized in Table 6 and it is interesting to note that all of the 'good' $Cl_2$ catalysts are also recognized good conductors. Given this it may at first appear surprising to note that both Pt and Au did not generate stoicheiometric yields of $Cl_2$. However, this is most likely due to rapid oxidation of the Pt and Au, by

some, or all (as appears to be the case for Au), of the chlorine generated. From Table 6, it also appears that $RuO_2 \cdot xH_2O$ can, after all, act as an efficient $Cl_2$ catalyst; no evidence was found to suggest that $RuO_4$ was generated *via* reaction 7.

It is worth noting at this point that the % $Cl_2$ yields for all the catalysts, including $RuO_2 \cdot xH_2O$, were determined by continuously sweeping out any $Cl_2$ generated in the reaction vessel using a stream of $N_2$ and subsequently passing the $N_2$ stream through a 'trap' solution containing a high concentration of $I^-$ ions. The amount of $Cl_2$ generated by the catalyst in the test system was then determined *via* the amount of tri-iodide found in the 'trap'.[52,59] As a consequence of this procedure, the $Cl_2$ concentration in the reaction vessel was always very low, thus making unlikely reaction 10 or, for that matter, any slow corrosion reaction involving the test 'redox catalyst' and $Cl_2$.

## 4 The Electrochemical Model of Redox Catalysis[18,19]

Before examining the observed kinetics for $O_2$ and $Cl_2$ redox catalysis mediated by $RuO_2 \cdot yH_2O$*, it is worth considering the likely implications of the electrochemical model of heterogeneous redox catalysis to either reaction. Both reactions 8 and 9 can be considered to be examples of a reversible couple (the reduction of $Ce^{IV}$ ions to $Ce^{III}$ ions) coupled to a comparatively highly irreversible reaction (*i.e.* the oxidation of water to $O_2$, or $Cl^-$ to $Cl_2$). For simplicity let us consider the kinetics of catalysis for this situation in terms of the general redox reaction 1, where $Ox_1/Red_1$ is the reversible couple used to oxidize the irreversible couple $Red_2/Ox_2$.

If the reduction of $Ox_1$ is electrochemically reversible at the redox catalyst then the cathodic current, $i_c$, will be related to the applied potential, $E_{ap}$, by the equation

$$E_{ap} = E_1' + (RT/n_1F) \ln \{(i_c - i_{1,c})/(i_{1,a} - i_c)\} \tag{11}$$

where $E_1'$ is the formal redox potential for the $Ox_1/Red_1$ couple and $i_{1,c}$ and $i_{1,a}$ are the limiting cathodic and anodic currents which reflect the maximum rates at which $Ox_1$ and $Red_1$, respectively, can be brought to the surface. Equation 11 assumes that mass transfer coefficients for $Ox_1$ and $Red_1$ are approximately the same and we shall refer to the value of this coefficient as $k_d$. The limiting cathodic and anodic currents can be calculated using the following equations

$$i_{1,c} = -n_1 F k_d A_{cat} [Ox_1] \tag{12}$$

and,

$$i_{1,a} = n_1 F k_d A_{cat} [Red_1] \tag{13}$$

where $A_{cat}$ is the effective catalyst surface area and $[Ox_1]$, $[Red_1]$ the concentrations of $Ox_1$ and $Red_1$, respectively.

[59] A. Mills and A. Cook, *Analyst (London)*, 1987, **112**, 1289.

If the oxidation of $Red_2$ is electrochemically irreversible at the redox catalyst then the anodic current, $i_a$, will be related to $E_{ap}$ by the equation

$$i_a = i_{0,2} \exp(1 - \alpha_2) z_2 F\eta / RT \tag{14}$$

provided the overpotential, $\eta$, is sufficiently large and positive and that the current–voltage curve lies in the Tafel region. In equation 14 $i_{0,2}$ is the exchange current, $\alpha_2$ is the cathodic transfer coefficient, $z_2$ is the number of electrons transferred in the rate determining step and, $\eta$ is the difference between $E_{ap}$ and the equilibrium potential for the $Ox_2/Red_2$ couple, $E_2$.

Assuming the Wagner–Traud additivity principle applies,[2] when both couples are present the redox catalyst particles will adopt a mixture potential ($E_{mix}$) at which the net current of the system is zero, *i.e.*

$$i_a = -i_c = i_{mix} \tag{15}$$

Under these conditions equation 11 may be written as

$$-i_c = \frac{n_1 k_d F A_{cat}([Ox_1] - [Red_1] \exp\{Fn_1(E_{mix} - E_1')/RT\})}{1 + \exp\{Fn_1(E_{mix} - E_1')/RT\}} \tag{16}$$

and equation 14 may be rewritten as

$$i_a = i_{0,2} \exp\{(1 - \alpha_2) z_2 F(E_{mix} - E_2')/RT\} \tag{17}$$

**A. Diffusion-controlled Kinetics.**—Diffusion-controlled kinetics will be observed when the mixture potential lies in the plateau region of the cathodic current–voltage curve for the $Ox_1/Red_1$ redox couple, as illustrated in Figure 6. The rate of reduction of $Ox_1$ will be proportional to $i_{mix}$ which, in turn, will be numerically equal to $i_{1,c}$. The relationship between $i_{1,c}$ and $[Ox_1]$ is given by equation 12, where $k_d$ is $D_{Ox1}/\delta$. $D_{Ox1}$ is the trace diffusion coefficient of $Ox_1$ in the supporting electrolyte and $\delta$ is the diffusion layer thickness. This latter parameter is a function of the hydrodynamic flow conditions around the redox catalyst and will be constant under fixed stirring conditions. A useful indication that the kinetics are diffusion-controlled is if the rate of disappearance of $[Ox_1]$ is first order with respect to $[Ox_1]$.

From equations 15—17 diffusion-controlled kinetics will be most likely to occur if $E_{mix}$ is near to $E_2$ and well away from $E_1$. This situation will be favoured if: (a) the equilibrium potentials of the two couples are well separated, (b) $i_{0,2}$ is large (although reaction 3 must still be irreversible), (c) there is a low concentration of $Ox_1$ and a high $[Ox_1]/[Red_1]$ ratio, and (d) the concentration $Red_2$ is high.

**B. Partly Diffusion-controlled Kinetics.**—This type of kinetics will be observed when $E_{mix}$ is typically 5—75 mV less than $E_1$, since under such conditions $i_{mix}$ will be $< 0.9 \times i_{1,c}$. The rate of reduction of $Ox_1$ under such conditions will be

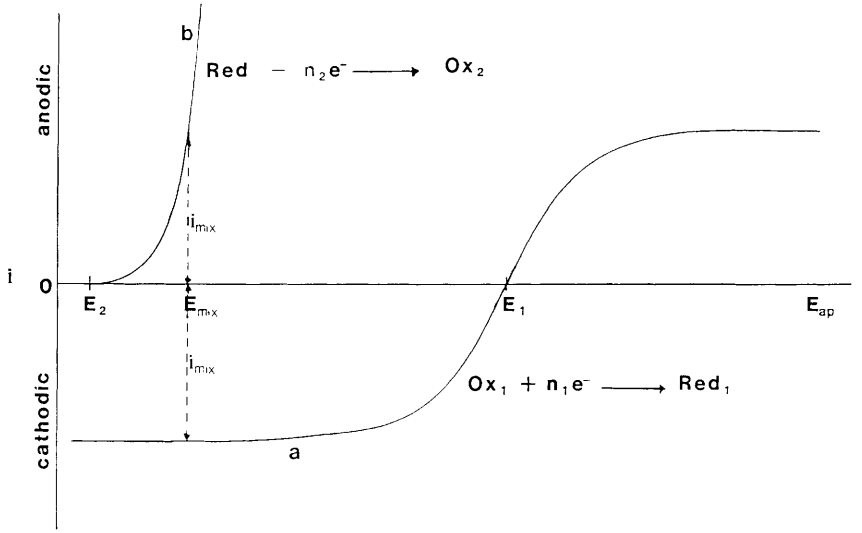


**Figure 6** *Schematic illustration of the current voltage curves for the reversible $Ox_1/Red_1$ couple (cathodic reaction, curve a) and the irreversible $Ox_2/Red_2$ couple (anodic reaction, curve b), when there is a large difference in equilibrium potentials and, as a result, $E_{mix}$ lies in the plateau region of curve a*

described by equations 15—17. A schematic illustration of this situation is given in Figure 7. A useful indication of this type of kinetics is if the rate of reduction of $Ox_1$ is *not* simply first order with respect to $[Ox_1]$ and decreases as $[Red_1]$ is increased. Such kinetics will often be expected if $E_2$ is close to $E_1$.

## 5 The Kinetics of $O_2$ and $Cl_2$ Catalysis

Despite the number and variety of reported examples of $O_2$ catalysts (see Table 2) there has been little attempt to study the kinetics of $O_2$ catalysis in any real detail, until the recent advent of a reproducible $O_2$ catalyst,[13,15] in the form of $RuO_2{\cdot}yH_2O$*. The same is also true for $Cl_2$ catalysts. One reason for this may have been the notorious irreproducibility[7,15] of such catalysts before the introduction of $RuO_2{\cdot}yH_2O$*. Another unredeeming feature of such work, which makes it initially appear unattractive and possibly complex, is the quite unusual situation of attempting accurate rate measurements of, say, the disappearance of the oxidizing agent in a dispersion of the catalyst. In practice, however, there are few difficulties, although care must be taken to thoroughly degrease all glassware prior to its use and it is useful to be able to disperse the catalyst using ultrasound.

We have recently carried out detailed studies of the kinetics of both reaction 8 and reaction 9 using $RuO_2{\cdot}yH_2O$* powder as the redox catalyst and $Ce^{IV}$ ions as the oxidant.[16,19,52] A schematic diagram of the experimental arrangement used is illustrated in Figure 8. As indicated in Figure 8 the kinetics of either redox-

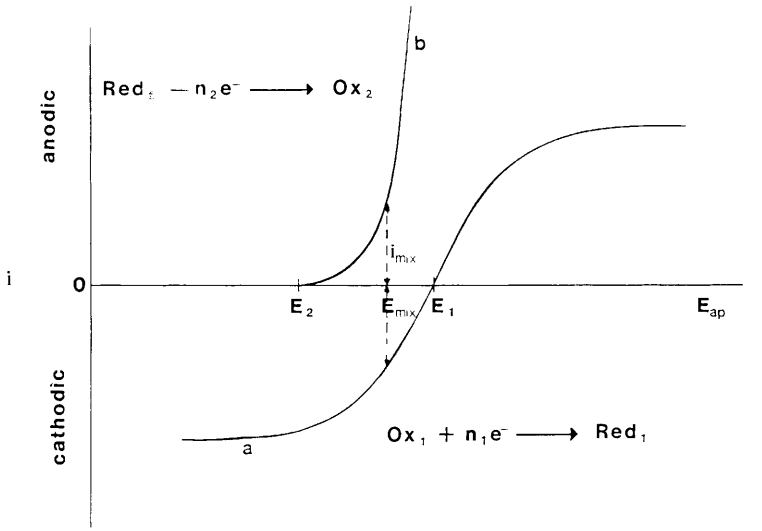


**Figure 7** *As in Figure 6, with the exception that the two current–voltage curves are not well separated and, consequently, $E_{mix}$ lies in a region of potential in which the current is less than diffusion-controlled*

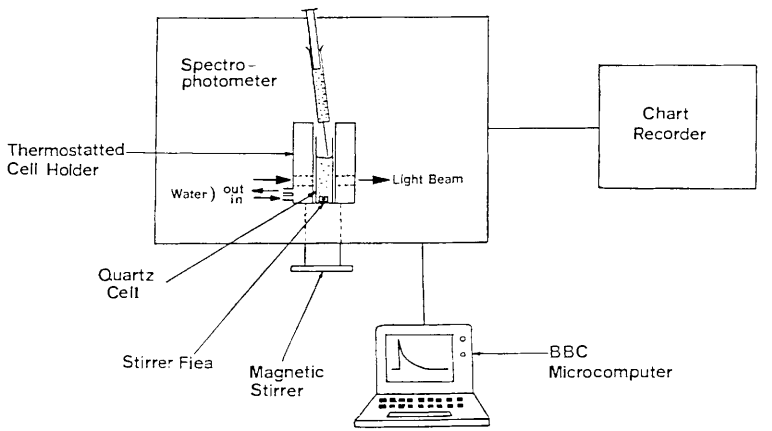


**Figure 8** *Schematic illustration of the system used to monitor the absorbance due to* $Ce^{IV}$ *ions* vs *time decay curves for both* $O_2$ *and* $Cl_2$ *catalysis*

catalysed reaction 8 or 9 were studied by monitoring spectrophotometrically the decrease in the concentration of $Ce^{IV}$ ions as a function of time. In a typical experiment 175 μg of $RuO_2 \cdot yH_2O$* were dispersed in a solution (2.5 $cm^3$) containing 0.5 mol $dm^{-3}$ $H_2SO_4$ (+2 mol $dm^{-3}$ NaCl for $Cl_2$ catalysis) which was contained in a 1 cm quartz cell. This dispersion was stirred continuously at

1 000 r.p.m. After 30 min, 90 $mm^3$ of a $Ce^{IV}$ solution (usually 0.1 mol $dm^{-3}$) were injected into the dispersion and the subsequent disappearance of the absorbance due to $Ce^{IV}$ ions (initial concentration after mixing 0.0036 mol $dm^{-3}$) was monitored spectrophotometrically at 430 nm ($\varepsilon$ = 290 $mol^{-1}$ $dm^3$ $cm^{-1}$) or, for low concentrations of $Ce^{IV}$ ions, 320 nm ($\varepsilon$ = 5 580 $mol^{-1}$ $dm^3$ $cm^{-1}$).

**A. $O_2$ Catalysis in $H_2SO_4$.**[19]—Using $RuO_2 \cdot yH_2O$* as the redox catalyst, the experimental system illustrated in Figure 8, and reaction conditions similar to those described in the previous paragraph, the kinetics of $Ce^{IV}$ reduction were found not to be simple first order and the rate appeared to decrease with increasing $Ce^{III}$ ion concentration. This inhibitory effect exhibited by $Ce^{III}$ ions on the kinetics of reaction 8 was observed most clearly in a series of experiments in which 100 $mm^3$ of a 0.1 mol $dm^{-3}$ $Ce^{IV}$ solution were injected into 2.8 $cm^3$ of a 0.5 mol $dm^{-3}$ $H_2SO_4$ solution containing different concentrations of $Ce^{III}$ ions, but always a fresh catalyst dispersion; after mixing (*ca.* 3 s) the initial $Ce^{IV}$ ion concentration ($[Ce^{4+}]_0$) was $3.45 \times 10^{-3}$ mol $dm^{-3}$. Figure 9a illustrates the variation of $[Ce^{4+}]$ as a function of time for a number of different initial $Ce^{IV}/Ce^{III}$ concentration ratios. As predicted by the electrochemical model this inhibitory effect of $Ce^{III}$ ions becomes less pronounced as the initial $[Ce^{4+}]$ is decreased. Thus for a $[Ce^{4+}]_0 = 3.45 \times 10^{-5}$ mol $dm^{-3}$ the decay curves recorded for a series of different $[Ce^{4+}]_0/[Ce^{3+}]_0$ ratios were very similar, as illustrated in Figure 9b. Considering the results of this initial study in the light of our electrochemical model of the system it would appear that the kinetics of reaction 8 are very near to diffusion-controlled at low $Ce^{IV}$ concentrations, *i.e.* $\leqslant 3.45 \times 10^{-5}$ mol $dm^{-3}$, and partly diffusion-controlled at high $Ce^{IV}$ concentrations, *i.e.* $\geqslant 3.45 \times 10^{-3}$ mol $dm^{-3}$.

(i) *Kinetics at Low $Ce^{IV}$ Concentrations.* A study of the kinetics of reaction 8 was carried out using an initial $[Ce^{4+}]$ and $[Ce^{3+}]$ of $3.45 \times 10^{-5}$ mol $dm^{-3}$ and 0 mol $dm^{-3}$, respectively.[19] The decay of the injected $Ce^{IV}$ ions obeyed first-order kinetics at least over the first half-life and provided a first-order diffusion-controlled rate constant, $k_m$. As noted previously from equation 12 of the electrochemical model, for a diffusion-controlled reaction the rate and therefore $k_m$, should be first order with respect to $[Ce^{4+}]$. In addition, from the electrochemical model the observed first-order rate constant, $k_m$, should depend directly upon the catalyst concentration, since $k_m = k_d A_{cat}$ and [catalyst] $\propto A_{cat}$. In order to test this, $k_m$ was determined as a function of [catalyst] over the range 0.02—0.2 g $dm^{-3}$. A plot of $\log(k_m/s^{-1})$ *vs.* $\log\{[\text{catalyst}]/(\text{g dm}^{-3})\}$ produced a good straight line {number of points ($n$) = 6; correlation coefficient ($r$) = 0.9981} with a gradient ($m$) = 1.14 $\pm$ 0.08. The near unity value of the gradient appears to confirm the prediction made by the model.

In another set of experiments using these dilute $Ce^{IV}$ solutions, $k_m$ was determined as a function of temperature over the range 20—70 °C. An Arrhenius plot of the results gave a good straight line and an activation energy of 17.2 $\pm$ 0.1 kJ $mol^{-1}$. The experimentally determined value of the activation

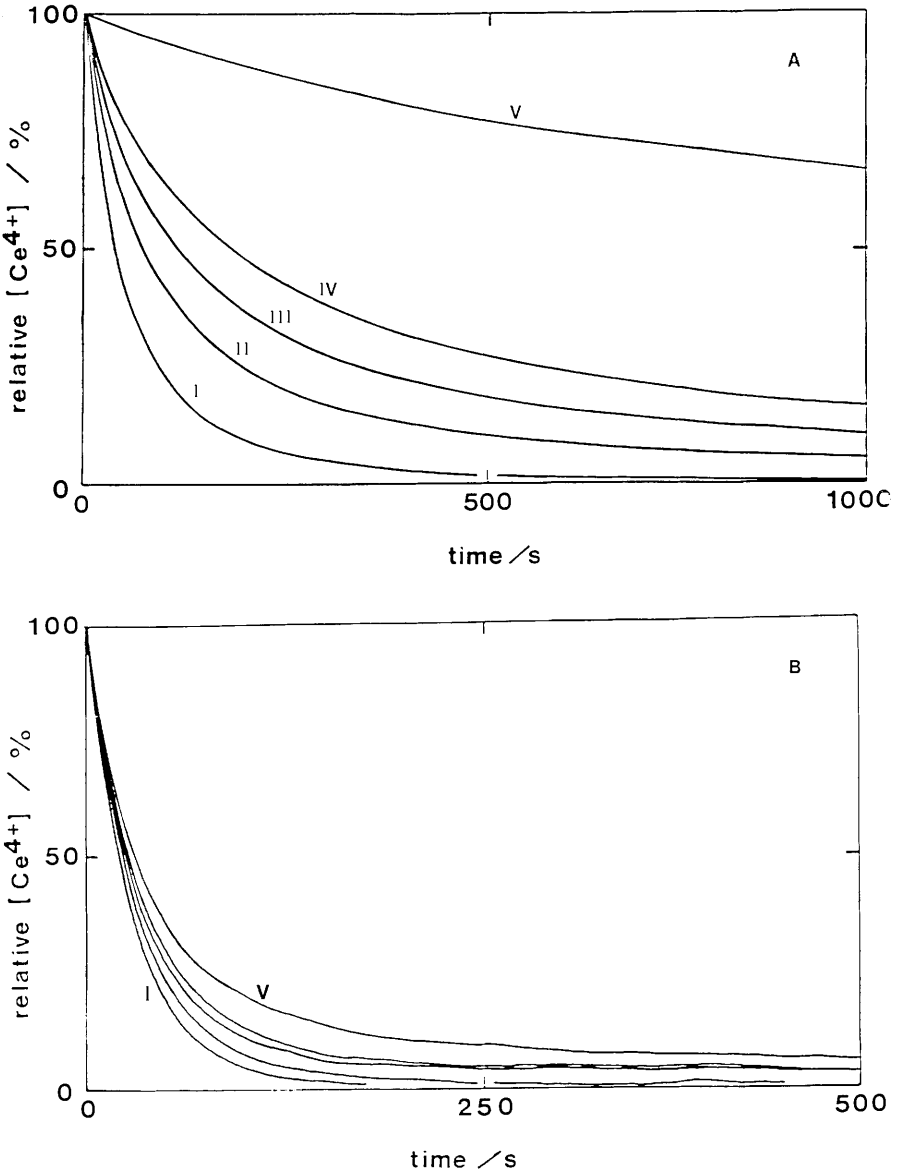


**Figure 9** *Observed variation of* $[Ce^{4+}]$ *as a function of time in which: (a) the initial* $[Ce^{4+}] = 3.45 \times 10^{-3}$ mol dm$^{-3}$ *and the initial* $Ce^{IV}/Ce^{III}$ *concentration ratios were* (i) 1:0, (ii) 1:1, (iii) 1:2, (iv) 1:3, *and* (v) 1:10, *respectively, and (b) the initial* $[Ce^{4+}] = 3.45 \times 10^{-5}$ mol dm$^{-3}$ *and the initial* $Ce^{IV}/Ce^{III}$ *concentration ratios were* (i) 1:0 (*fastest*), (ii) 1:1, (iii) 1:2, (iv) 1:3, and (v) 1:9 (*slowest*), *respectively. The concentration of* $RuO_2 \cdot yH_2O$* *was* 0.086 g dm$^{-3}$

reaction compares very well with that expected[60,61] for a diffusion-controlled reaction, *i.e.* 15—19 kJ $mol^{-1}$, and provides further support for the suggestion that at concentrations of $Ce^{IV} \leqslant 3.45 \times 10^{-5}$ mol $dm^{-3}$ the kinetics of reaction 8 are diffusion-controlled.

As noted above the first-order rate constant, $k_m$, is equal to $k_d A_{cat}$ where $k_d$ is its *heterogeneous* counterpart, the mass transfer coefficient. Since $k_m$ is a measurable quantity and the surface area of the redox catalyst used in this study is also known (87 $m^2$ $g^{-1}$, determined using a BET technique), it follows that a value for $k_d$ can be calculated. From the results of our kinetic study of reaction 8 at low $Ce^{IV}$ concentrations $k_d$ was estimated as $4.4 \times 10^{-4}$ cm $s^{-1}$. We shall use this value of $k_d$ later on in the article (see Section 5Aiii).

(ii) *Kinetics at High* $Ce^{IV}$ *Concentrations.*[19] The rate of reduction of $Ce^{IV}$ ions *via* reaction 8 observed at high initial concentration of $Ce^{IV}$ ions ($3.45 \times 10^{-3}$ mol $dm^{-3}$) appeared to decrease as the initial concentration of $Ce^{III}$ ions was increased, see Figure 9a. As suggested earlier, this trend is expected if the kinetics are partly diffusion-controlled and described by equations 15—17 of the electrochemical model.

For any decay trace the rate of reduction of the $Ce^{IV}$ ions, at any time $t$, is $r(t)$ (units: mol $cm^{-3}$ $s^{-1}$), where $r(t) = d[Ce^{4+}]_t/dt$. This rate is related directly to $i_{mix}$ by the expression

$$r(t) = i_{mix}/F \tag{18}$$

Since we are dealing with a heterogeneous system it is more appropriate to discuss the kinetics in terms the rate of a chemical surface reaction $\{i.e.\ R_{mix}(t)\}$, which has units of mol $cm^{-2}$ $s^{-1}$. This heterogeneous rate is related to $i_{mix}$ and $r(t)$ as follows:

$$R_{mix}(t) = i_{mix}/FA_{cat} = r(t)/A_{cat} \tag{19}$$

In our work on the kinetics of reaction 8 both the initial concentrations of $Ce^{IV}$ and $Ce^{III}$ ions are known. Thus, by monitoring the disappearance of the $Ce^{IV}$ ions as a function of time, we can obtain both $[Ce^{4+}]_t$ and $[Ce^{3+}]_t$ at any time, $t$. From $r(t)$, the derivative of the $[Ce^{4+}]$ *vs.* time curve at time $t$ we can also determine $i_{mix,t}$ and $R_{mix}(t)$, *via* equations 18 and 19. A knowledge of $R_{mix}(t)$ then allows us to calculate the mixture potential at time $t$ (*i.e.* $E_{mix,t}$) at the $RuO_2 \cdot yH_2O$* microelectrode particles, using a modified and rearranged version of equation 17, *i.e.*

$$E_{mix,t} = E^{\circ}_{Ce} + RT/F \ln \{(-k_d[Ce^{4+}]_t - R_{mix}(t))/(R_{mix}(t) - k_d[Ce^{3+}]_t)\} \tag{20}$$

provided $k_d$ is known.

[60] F. Wilkinson, 'Chemical Kinetics and Reaction Mechanisms,' Van Nostrand Reinhold, London, 1981, p. 140.
[61] J. W. Moore and R. G. Pearson, 'Kinetics and Mechanism, J. Wiley, New York, 1981, p. 239.

In the example of redox catalysis we are considering the redox couple $Ox_2/Red_2$ is really the $O_2/H_2O$ couple and equation 14 can be rewritten as follows

$$i_a = i_w \exp(2.303 \times \eta/b) \tag{21}$$

where, $i_w$ is the exchange current for the $O_2/H_2O$ couple on the $RuO_2{\cdot}yH_2O$* powder particles, $b$ is the Tafel slope and $\eta$ is the difference between $E_{ap}$ and the equilibrium potential for the $O_2/H_2O$ couple ($E_w$ is taken to be 1.23 V *vs.* NHE). It follows that a major prediction of this type of kinetics is that a plot of $E_{mix,t}$ *vs.* log $\{R_{mix}(t)\}$ should produce a straight line of gradient $b$ and intercept $-b \times \log(R_w)$, where

$$R_w = [i_w \exp(-2.303 \times E_w/b)]/FA_{cat} \tag{22}$$

For each of the decay curves illustrated in Figure 9a we were able to calculate for a variety of different times, $t$, covering the span (>3 half-lives) of each of the decay curves, both $R_{mix}(t)$, using equation 19 and the derivative, $r(t)$, and $E_{mix,t}$, using equation 20 and a value for $k_d$ of $4.4 \times 10^{-4}$ cm $s^{-1}$. As predicted by the electrochemical model, for each decay curve a plot of $E_{mix,t}$ *vs.* log $\{R_{mix}(t)\}$ produced a straight line with a common gradient and intercept; these plots are illustrated in Figure 10. A least squares analysis of the data illustrated in Figure 10, produced the following information: $n = 80$, $r = 0.9968$, $b = 0.0309 \pm 0.0005$ V/decade, $-b \times \log(R_w) = 1.708 \pm 0.006$ V. From the values for the intercept and gradient the exchange current density, $i_w/A_{cat}$, (units: A $cm^{-2}$) for the oxidation of water on the surface of the $RuO_2{\cdot}yH_2O$* powder particles can be calculated as *ca.* $(3.45 \pm 0.03) \times 10^{-11}$ A $cm^{-2}$, using equation 22. At mixture potentials <1.36 V there was evidence to suggest that the Tafel slope $b$, and therefore possibly the mechanism, for water oxidation had changed. As a result, the current exchange density calculated above was only a formal quantity and the true value may well be considerably smaller.

The oxidation of water to oxygen at the electrode surface may occur *via* the 'oxide pathway',[62] i.e.

$$S + H_2O \longrightarrow S\text{–}OH + H^+ + e^- \tag{23}$$

$$2S\text{–}OH \longrightarrow S\text{–}O + S + H_2O \tag{24}$$

$$2S\text{–}O \longrightarrow 2S + O_2 \tag{25}$$

where S is the surface active site. It can be shown that if reaction 23, 24, or 25 is the rate determining step then the Tafel slope will be 120, 30 or 15 mV, respectively. Thus, we can interpret our observed Tafel slope of 30.9 mV/decade in terms of the 'oxide pathway', where reaction 24 is the rate determining step.

[62] J. O'M. Bockris, *J. Chem. Phys.*, 1956, **24**, 817.

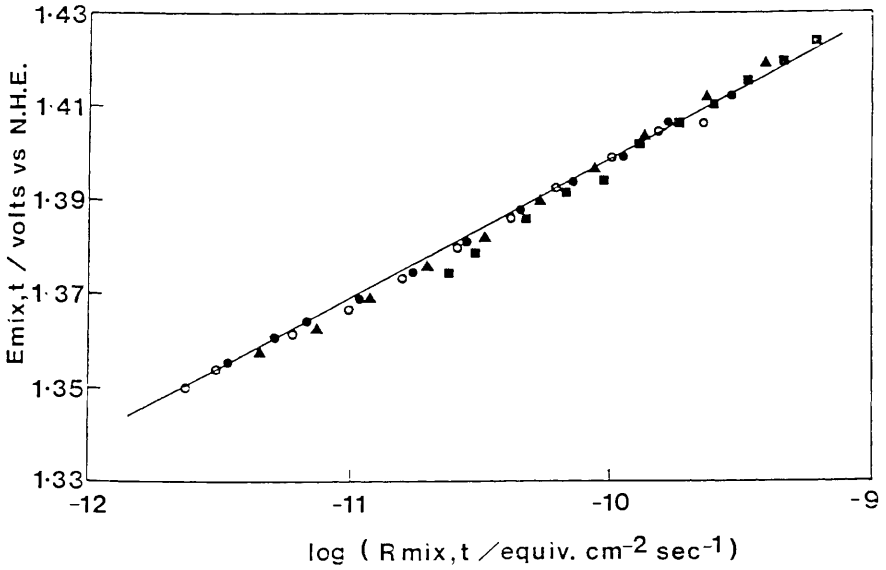


**Figure 10** *Tafel plot of* $E_{mix,t}$/(V vs. *NHE*) vs. log ($R_{mix,t}$/equiv. cm $^{-2}$ $s^{-1}$). *The data used to construct this plot were taken from Figure* 9a *curves* (i) ■, (ii) ▲, (iii) ●, and (iv) ○

Interestingly, a number of electrochemical studies of the oxidation of water to $O_2$ have been carried out using high defect hydrous ruthenium dioxide anodes,[63] a material which is likely to have similar electrochemical characteristics to $RuO_2 \cdot yH_2O$*. In most cases the Tafel slope was also found to be 30 mV/decade and, coupled with other findings, was invariably interpreted, as we have done, in terms of the oxide pathway, with reaction 24 as the rate determining step.[64,65]

A series of [$Ce^{4+}$] decay curves were recorded for a variety of catalyst concentrations over the range 0.02—0.2 g $dm^{-3}$. A plot of $E_{mix,t}$ *vs.* log $\{r(t) \times V_s\}$, where $V_s$ = the volume of solution in the reaction cell, was made for each of the decay curves and the resulting collection of straight lines is illustrated in Figure 11. Using the data in Figure 11 a plot of log $\{r(t) \times V_s\}$ *vs.* log [redox catalyst] was made for three different set potentials, *i.e.* 1.40, 1.38, and 1.36 V *vs.* NHE. The product was three, almost parallel, straight lines with a mean value for the gradient of *ca.* 1.25 ± 0.05. This finding supports the electrochemical model which predicts that $r(t)$ will depend directly upon $A_{cat}$ and, therefore, directly upon [redox catalyst] (see equation 19).

The activation energy of water oxidation reaction was determined *via* a set of

[63] S. Trasatti and W. E. O'Grady, *Adv. Electrochem. Electrochem. Eng.* 1981, **12**, 180, and references therein.
[64] G. Lodi, E. Sivieri, A. de Battisti, and S. Trasatti, *J. Appl. Electrochem.*, 1978, **8**, 135.
[65] S. Trasatti and G. Lodi, 'Electrodes of Conductive Metallic Oxides,' ed. S. Trasatti, Elsevier, Amsterdam, 1980, Chapter 10 and references therein.

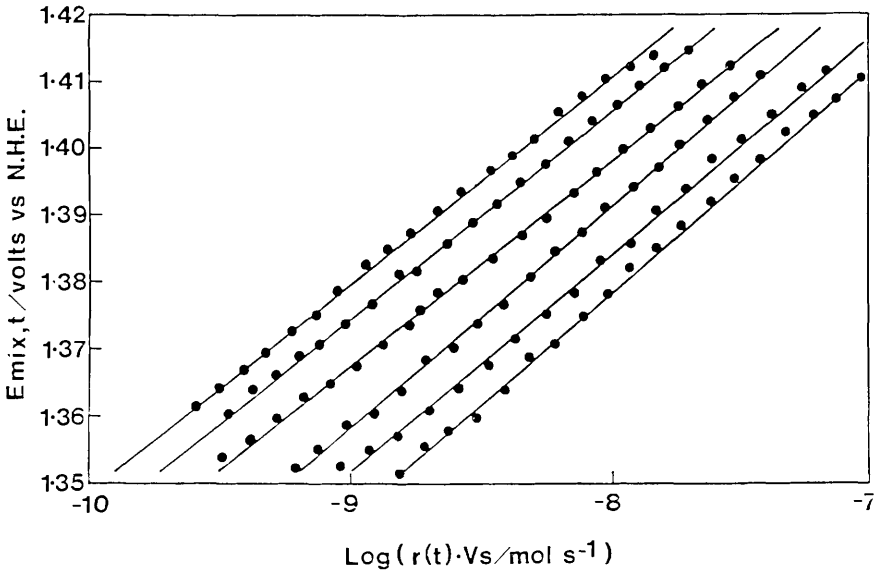


**Figure 11** *Tafel plot of* $E_{mix,t}$/(V vs. *NHE*) vs. log $\{r(t) \times V_s/\text{mol s}^{-1}\}$ *for a series of different catalyst concentrations. From left to right the plots correspond to a redox catalyst concentration of:* 21.8, 32.7, 49.0, 73.6, 110.3, *and* 165.5 mg $dm^{-3}$, *respectively. In this work the initial* $[Ce^{4+}]$ *was* 3.45 × $10^{-3}$ mol $dm^{-3}$ *and the initial* $Ce^{IV}/Ce^{III}$ *ratio was* 1:1

experiments conducted over the temperature range 20—70 °C using an initial $Ce^{IV}$ concentration of 3.45 × $10^{-3}$ mol $dm^{-3}$, a $[Ce^{4+}]_0/[Ce^{3+}]_0$ ratio of 1:4 and a redox catalyst concentration of 0.08 g $dm^{-3}$. The $Ce^{IV}$ decay curves recorded at each temperature were analysed over three half-lives and used to generate a set of $E_{mix,t}$ *vs.* log $\{R_{mix}(t)\}$ data. At mixture potentials >1.36 V *vs.* NHE all the Tafel plots of this data are straight lines with an approximately common slope (*ca.* 30.1 mv/decade). However, at $E_{mix,t}$ < 1.36 V *vs.* NHE a deviation to a lower Tafel slope value is apparent, indicating, possibly, a change of mechanism at these low overpotentials. This can be rationalized in terms of the oxide pathway mechanism, since, as the potential on the $RuO_2 \cdot yH_2O^*$ particles falls, so will the surface coverage of S–O species. Eventually a point may be reached when reaction 25 becomes rate limiting and, as a result, the Tafel slope will be expected to change to 15 mV/decade.[62,63]

Arrhenius plots were constructed by taking the rate value from each Tafel plot at a series of fixed potentials, 1.40, 1.38, and 1.36 V *vs.* NHE, respectively. From the gradients of the three approximately parallel straight lines a mean activation energy for the oxidation of water to $O_2$ on the surface of the $RuO_2 \cdot yH_2O^*$ particles was calculated to be 52 ± 8 kJ $mol^{-1}$. This value for the activation energy compares favourably with the value of 50.4 kJ $mol^{-1}$, determined previously by another group,[64] in a macroelectrode study of the oxidation of water using a hydrous ruthenium dioxide anode.

(iii) *Simulation of the* $Ce^{IV}$ *Decay Curves.*[18,19] The pertinence of the electrochemical model used here, its assumptions, mathematical description, and the accuracy of our analysis based upon the model are best assessed by the solution and integration of equations 20 and 21 in conjunction with our estimated values for the constants involved; these constants include: $R_w = 2.69 \times 10^{-16}$ equiv. $cm^{-2}$ $s^{-1}$, $b = 30$ mV/decade (both calculated from the data in Figure 10, for $E_{mix}$ values $> 1.36$ V *vs.* NHE) and $k_d = 4 \times 10^{-4}$ cm $s^{-1}$. Using Newton's method and the combination of equations of 20 and 21 it can be shown that for any known values of $[Ce^{4+}]_0$ and $[Ce^{3+}]_0$ the mixture potential on the particle can be determined, $E_{mix}$, which, in turn, can be used to calculate $i_{mix}$ using equation 21.[18] Provided the initial concentrations of $Ce^{IV}$ and $Ce^{III}$ ions are known, this routine coupled to a variable step version of Euler's method may be combined to regenerate any of the observed $[Ce^{4+}]$ *vs.* time decay curves and used to predict the shapes of decay traces under very different reaction conditions. A detailed description of the procedure has been given in a previous paper.[18]

Figures 12a and 12b illustrate reconstructed versions of the decay curves given in Figures 9a and 9b, respectively. The fit to the experimentally determined decay curves at $[Ce^{4+}]_0 = 3.45 \times 10^{-3}$ mol $dm^{-3}$ is very good but at $[Ce^{4+}]_0 = 3.45 \times 10^{-5}$ mol $dm^{-3}$ the experimental curves are marginally, but consistently, faster than the simulated curves. There is evidence to suggest that this may be due to the non-steady state process of catalyst charging, which occurs when the $Ce^{IV}$ ions and the catalyst are first mixed. It can be shown[17] that this process will only make a significant contribution to the observed decay of the $Ce^{IV}$ ions when their concentration is very low, *i.e.* $\leqslant 3.45 \times 10^{-5}$ mol $dm^{-3}$.

**B. $O_2$ Catalysis in $HClO_4$.**[16]—From our interpretation of the kinetics of reaction 8 using the electrochemical model it appears that in 0.5 mol $dm^{-3}$ $H_2SO_4$ and high concentrations of $Ce^{IV}$ ions the current–voltage curves are not well separated and the rate of reduction of $Ce^{IV}$ ions is partly diffusion-controlled. However, at low concentrations of $Ce^{IV}$ ions in the same acid medium the kinetics appear close to diffusion-controlled and this result suggests that if the separation between the equilibrium potentials of the $Ce^{IV}/Ce^{III}$ and $O_2/H_2O$ couples could be increased in some way, by 50—100 mV say, then the kinetics at high $Ce^{IV}$ concentrations should become wholly diffusion-controlled. Now, although the formal redox potential (which provides a measure of the equilibrium potential) of the $Ce^{IV}/Ce^{III}$ couple is 1.44 V *vs.* NHE in 0.5 mol $dm^{-3}$ $H_2SO_4$, it is 1.70 V *vs.* NHE in 2 mol $dm^{-3}$ $HClO_4$. Thus an increased separation in equilibrium potentials can be achieved by carrying out the reaction in a medium containing 1 mol $dm^{-3}$ $HClO_4$ and little (or no) $H_2SO_4$.

In practice it was found to be easier to work with an acid medium which was predominantly $HClO_4$, *i.e.* 1 mol $dm^{-3}$ $HClO_4$ + $3.5 \times 10^{-2}$ mol $dm^{-3}$ $H_2SO_4$. In this medium the formal potential of the $Ce^{IV}/Ce^{III}$ couple was measured as 1.58 V *vs.* NHE, 140 mV more positive than that in 0.5 mol $dm^{-3}$ $H_2SO_4$. As indicated by the results contained in Table 7, $RuO_2 \cdot yH_2O$* is able to mediate the stoicheiometric oxidation of water to $O_2$ by $Ce^{IV}$ ions in this predominantly $HClO_4$ medium and exhibits no evidence of anodic corrosion.

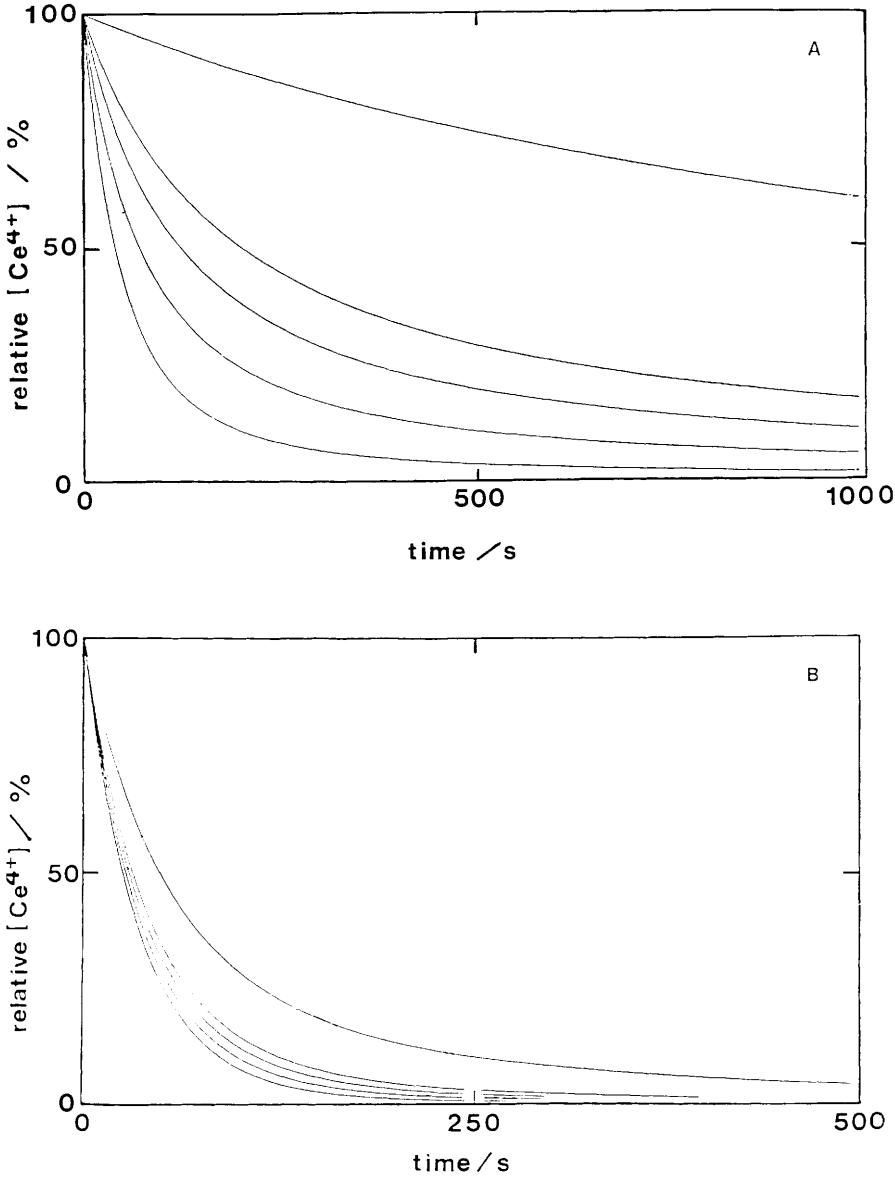


**Figure 12** *Digitally simulated curves for initial* $Ce^{IV}$ *ion concentrations of* (*a*) $3.45 \times 10^{-3}$ *and* (*b*) $3.45 \times 10^{-5}$ mol $dm^{-3}$. *These decay curves were reconstructed using equations* 20 *and* 21 *as outlined in Section* 5Aiii. *The assumed initial reaction conditions were identical to those used in generating the observed decay curves illustrated in Figures* 9a *and* 9b

**Table 7** *% $O_2$ yields and % corrosion for* $RuO_2{\cdot}yH_2O$* *in different acid media* ($T$ = 298 K)

| *Acid Medium* | *% $O_2$ Yield* | *% Corrosion* |
|---|---|---|
| 0.5 mol $dm^{-3}$ $H_2SO_4$ | 97 | 0 |
| 1 mol $dm^{-3}$ $HClO_4$ + 3.5 × $10^{-2}$ mol $dm^{-3}$ $H_2SO_4$ | 91 | 0 |

In one set of experiments the initial concentration of $Ce^{IV}$ ions was systematically varied over the range 3.5 × $10^{-3}$ to 3.9 × $10^{-5}$ mol $dm^{-3}$ and for each recorded decay trace case the first-order plot gave an excellent straight line ($r \geqslant 0.9999$)! From this work an average value for $k_m$ was determined as 4.8 × $10^{-2}$ $s^{-1}$. Further kinetic studies established that $k_m$ was proportional to the catalyst concentration and independent of the initial concentration of $Ce^{III}$ ions. From the measured variation of $k_m$ with temperature, in 1 mol $dm^{-3}$ $HClO_4$ + 3.5 × $10^{-2}$ mol $dm^{-3}$ $H_2SO_4$, the activation energy for reaction 8 was determined as 22 kJ $mol^{-1}$. All these results are as predicted by equation 12 of the electrochemical model and indicate that the reduction of $Ce^{IV}$ ions *via* reaction 8 in 1 mol $dm^{-3}$ $HClO_4$ + 3.5 × $10^{-2}$ mol $dm^{-3}$ $H_2SO_4$ are diffusion-controlled.

**C. Kinetics of $Cl_2$ Catalysis.**[52]—As noted earlier and illustrated in Figure 5, when $RuO_2{\cdot}yH_2O$* is used as the redox catalyst for reaction 9, the % yield of $Cl_2$ evolved increases as the $Cl^-$ ion concentration is increased. At $Cl^-$ concentrations $>0.2$ mol $dm^{-3}$ stoicheiometric amounts of $Cl_2$ are generated. Thus, in order to ensure that in our kinetic study the reduction of $Ce^{IV}$ ions was due to reaction 9, rather than reaction 8, the concentration of $Cl^-$ ions used was always 2 mol $dm^{-3}$, unless stated otherwise.

The kinetics for the reduction of $Ce^{IV}$ ions *via* reaction 9 were studied as a function of initial $Ce^{IV}$ concentration over the range 3.6 × $10^{-3}$—3.6 × $10^{-4}$ mol $dm^{-3}$. In all cases, the observed decay curves, analysed over at least two half-lives, produced excellent straight lines ($r \geqslant 0.9997$) when plotted out in the form $\ln(\Delta A)$ *vs.* $t$. These results indicate that the rate of reduction of $Ce^{IV}$ ions in reaction 9 is first-order with respect to $[Ce^{4+}]$.

Further work on the kinetics of $Ce^{IV}$ reduction established that the first-order rate constant, $k_m$, was independent of the initial concentration of $Ce^{III}$ ions and directly dependent upon the redox catalyst concentration. In addition $k_m$ was determined as a function of temperature and from the resulting Arrhenius plot of the data an activation energy of 27 ± 4 kJ $mol^{-1}$ was estimated for reaction 9. Taken as a whole the results of the kinetic study indicate that the reduction of $Ce^{IV}$ ions is diffusion-controlled, although the experimentally determined value for the activation energy was slightly higher than might be expected for a diffusion-controlled reaction.[60,61]

We have already noted (see section 5A) that for reaction 8, in 0.5 mol $dm^{-3}$ $H_2SO_4$, the kinetics of $Ce^{IV}$ reduction are diffusion-controlled only when the initial $Ce^{IV}$ concentration is low (*i.e.* $\leqslant 3.45 \pm 10^{-5}$ mol $dm^{-3}$), despite the quite large separation between the standard redox potentials for the $Ce^{IV}/Ce^{III}$ and

$O_2/H_2O$ redox couples, $\Delta E(O_2) = 220$ mV, see Table 3. As a result, it might at first appear unlikely that the kinetics for reaction 9 would be diffusion-controlled at high or low $Ce^{IV}$ concentrations, as has been found, given that the reaction medium was also 0.5 mol $dm^{-3}$ $H_2SO_4$ and therefore $\Delta E(Cl_2)$ was only +90 mV, *i.e.* 130 mV less than $\Delta E(O_2)$.

To rationalize our observations we must first consider the current–voltage curve for the oxidation of chloride to $Cl_2$ which, like that of water (see equation 21), will most likely be best described by a Tafel equation,[66] *i.e.*

$$i_{Cl_2} = i_{0,Cl} \exp(2.303 \times b^* \eta^*) \tag{26}$$

where $i_{0,Cl}$ is the exchange current for the $Cl_2/Cl^-$ couple on the $RuO_2 \cdot yH_2O^*$ powder particles, $b^*$ is the Tafel slope, and $\eta^*$ is the difference between $E_{ap}$ and the equilibrium potential for the $Cl_2/Cl^-$ couple ($E^0_{Cl}$). In contrast with the electrochemical oxidation of water to $O_2$, the oxidation of $Cl^-$ to $Cl_2$ is classed as 'facile' for most electrodes, *i.e.* insensitive to the fine structure of the electrodes surface, and usually associated with an exchange current which is much greater than that for water, *e.g.* for $RuO_2$ electrodes[65] $i_{0,Cl} \geqslant 10^{-4}$ A $cm^{-2}$ and $i_w \leqslant 10^{-7}$ A $cm^{-2}$. As indicated in section 4.1 a high exchange current density will favour diffusion-controlled kinetics since in this situation it is likely that $E_{mix}$ will be close to $E_{Cl}$ and well removed from the equilibrium potential of the $Ce^{IV}/Ce^{III}$ couple, $E_{Ce}$. Thus, in 0.5 mol $dm^{-3}$ $H_2SO_4$, although the separation of the equilibrium potentials for the $Ce^{IV}/Ce^{III}$ and $Cl_2/Cl^-$ couples is much less than that for the $Ce^{IV}/Ce^{III}$ and $O_2/H_2O$ couples the observation of diffusion-controlled kinetics in the former system arises because $i_{0,Cl} \gg i_w$.

In our study of reaction 9 mediated by $RuO_2 \cdot yH_2O^*$ we examined the effect on the rate of $Ce^{IV}$ reduction as a function of $Cl^-$ concentration. Interestingly, for low concentrations of $Ce^{IV}$ ions, $k_m$ was found to be independent of $Cl^-$ concentration not only over the $[Cl^-]$ range 2—0.2 mol $dm^{-3}$, where $Cl_2$ is the sole gaseous product, but also over the $[Cl^-]$ range 0.2—0.01 mol $dm^{-3}$ where the % $Cl_2$ yield drops to 0% and the % $O_2$ yield rises to 100%. Thus it appears that the rate of reduction of $Ce^{IV}$ ions is, in the case of water and $Cl^-$ oxidation, *independent of the product* (i.e. $O_2$ *and* $Cl_2$) *being formed.* This is as predicted by the electrochemical model since we have established that under the reaction conditions employed both reactions 8 and 9 are diffusion-controlled and, therefore, the mixture current will be equal to $i_{1,c}$ (equation 12, where $[Ox_1] = [Ce^{4+}]$) and independent of $Cl^-$ concentration. As a result, the mixture current may be expressed as

$$i_{mix} = i_{Cl_2} + i_{O_2} = \text{constant} \tag{27}$$

If $\theta$ is the order that $i_{o,Cl}$ depends upon $[Cl^-]$, then we can expect the % $Cl_2$

[66] W. J. Albery, P. N. Bartlett, and A. J. McMahon in 'Photogeneration of Hydrogen,' ed. A. Harriman and M. A. West, Academic Press, London, 1982, p. 85.

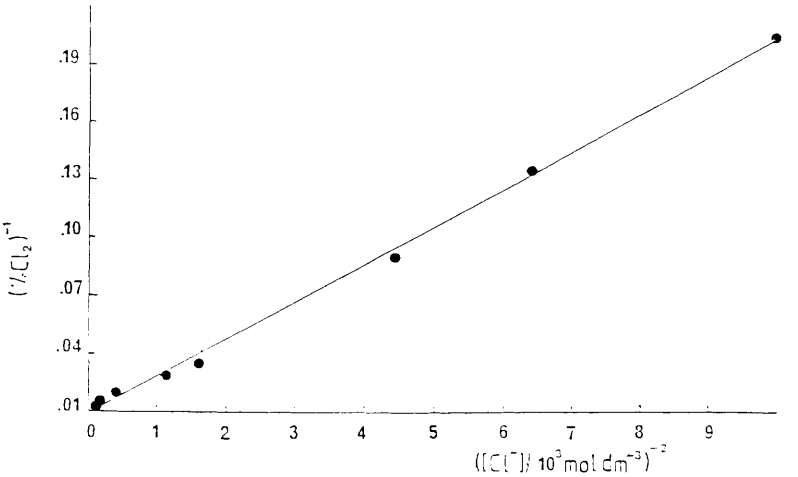


**Figure 13** *Plot of* $1/(\%\ Cl_2\ yield)$ vs. $[Cl^-]^{-2}$ *using the data illustrated in Figure 5*

yield observed for a chloride concentration, $[Cl^-]$ to be given by the expression

$$\%\ Cl_2 = 100K\{[Cl^-]^\theta \exp(2.303b^*\eta^*)\}/\{K[Cl^-]^\theta \exp(2.303b^*\eta^*) + i_w \exp(2.303b\eta)\} \quad (28)$$

where $K$ is a proportionality constant. This expression simplifies significantly if we make the assumption that the two Tafel slopes, $b^*$ and $b$, are similar, *i.e.* $b^* \simeq b$. This assumption is not too unlikely given that we have established $b =$ 30 mV, and work on $RuO_2$ based electrodes has established[65] that $b^*$ is usually also 30 mV. Using this assumption we can simplify equation 28 to

$$1/\%\ Cl_2\ yield = 0.01 + \{Z\exp(b[\eta - \eta^*])\}/[Cl^-]^\theta \quad (29)$$

where, $Z$ is $0.01 \times i_w/K$. The term $[\eta - \eta^*]$ is the difference between the equilibrium potentials of the two redox couples and, therefore, is a constant. A plot of the data illustrated in Figure 5 in the form of $1/\%\ Cl_2$ yield *vs.* $[Cl^-]^{-2}$ is illustrated in Figure 13 and is a good straight line ($r = 0.9988$). These results suggest that $i_{0,Cl}$ depends upon the square of the chloride ion concentration, *i.e.* $\theta = 2$.

The two mechanisms for the electrochemical oxidation of $Cl^-$ to $Cl_2$ proposed most often are (a) the Volmer–Tafel mechanism with two steps: the Volmer reaction

$$Cl^- \longrightarrow Cl_{ad} + e^- \quad (30)$$

and the Tafel reaction

$$2Cl_{ad} \longrightarrow Cl_2 \quad (31)$$

**Table 8** *Preparation of colloids of hydrated ruthenium*(IV) *oxide*

| *Preparation* | *Protecting Agent* | *Ref.* |
|---|---|---|
| Reduction of $RuO_4$ by the polybrene | Polybrene | 21,22 |
| Reduction of $RuO_4^-$ by $H_2O_2$ | Styrene/maleic anhydride co-polymer | 23 |
| Reduction of $RuO_4^-$ *via* gamma radiolysis | None | 23 |
| Reduction of $RuO_4^-$ by $H_2O_2$ | None | 26 |
| Reduction of hydrated $RuO_4$ by the protecting agent and water | Styrene/maleic anhydride co-polymer | 28,35 |
| Reduction of $RuO_4^{2-}$ by water and, possibly, SDS | SDS | 34 |
| Reduction of $RuO_4^{2-}$ by water and, possibly, PVP | PVP | 34 |
| Reduction of $RuO_4$ by water onto colloidal $TiO_2$ | — | 39 |

Polybrene = 1,5-dimethyl-1,5-diazaundecamethylene polymethobromide, hexadimethrine bromide. SDS = sodium dodecyl sulphate. PVP = poly(vinyl pyridine)

and (b) the Volmer–Heyrovsky mechanism, comprising the Volmer reaction 30 and the Heyrovsky reaction

$$Cl^- + Cl_{ad} \longrightarrow Cl_2 + e^- \qquad (32)$$

It can be calculated that in our work the current density flowing through the $RuO_2{\cdot}yH_2O$* particles is low, typically $<0.025$ mA $cm^{-2}$. In both the above reaction mechanisms the current would be expected to be second order with respect to the $Cl^-$ concentration at low current densities if the second steps (reactions 31 and 32) were rata-determining. However, it should be noted that under such conditions the Tafel slopes for the two mechanisms would be different, *i.e.* 29.6 and 39.5 mV, respectively. As indicated previously, in most studies using $RuO_2$-based macroelectrodes $b$* is usually found[66] to be 30 mV and interpreted in terms of the Volmer–Tafel mechanism. The results of our kinetic study of reaction 9 mediated by $RuO_2{\cdot}yH_2O$* appear entirely consistent with those predicted using an electrochemical model of redox catalysis, in which the oxidation of $Cl^-$ to $Cl_2$ occurs *via* a Volmer–Tafel mechanism (reactions 30 and 31) with reaction 31 as the slowest of the two steps.

## 6 Colloidal Catalysts

In the search for faster-acting $O_2$ catalysts a number of research groups have reported the preparation of different colloids of hydrated ruthenium(IV) oxide and their application as $O_2$ catalysts (see Tables 2 and 8). To our knowledge, however, no colloidal $Cl_2$ catalysts have been reported. In general, most of the colloids of hydrated ruthenium(IV) oxide have been poorly characterized with the consequence that little is known about the degree of hydration of the ruthenium(IV) oxide. This is unfortunate given its proven relevance to corrosion stability and catalytic activity (see Figure 4).[14,15]

Unlike powder dispersions, colloids of hydrated ruthenium(IV) oxide are usually optically clear. As a result, the kinetics of $O_2$ catalysis by such colloids are more easily studied using spectrophotometric techniques than those for

powders. However, surprisingly few detailed kinetic studies have been carried out. In addition, when colloids of hydrated ruthenium(IV) oxide have been used as $O_2$ catalysts there has often been no attempt to look for and quantify the degree of anodic corrosion undergone by the catalyst, despite its relevance in assessing catalyst stability. In the few examples in which the % corrosion was measured,[21,23] usually using $Ce^{IV}$ ions as the oxidant, it was found to be significant, *i.e.* 27—40%. Indeed, for some colloids at least, it appears that even the mild oxidant $Ru(bpy)_3^{3+}$ is able to corrode hydrated ruthenium(IV) oxide to $RuO_4$.[23,26]

Grätzel and his co-workers[39] have carried out a study of the kinetics of water oxidation by photochemically generated $Ru(bpy)_3^{3+}$ mediated by hydrated ruthenium(IV) oxide deposited onto colloidal particles of $TiO_2$. The kinetics were monitored spectrophotometrically, *via* the decrease in absorbance due to the photogenerated $Ru(bpy)_3^{3+}$ species, and conductiometrically *via* the increase in solution conductance due to the generation of protons through the oxidation of water. The decay of the $Ru(bpy)_3^{3+}$ absorbance and the increase in conductivity were always found to occur concomitantly and with the correct stoicheiometry expected for the oxidation of water by $Ru(bpy)_3^{3+}$. These findings have been taken as direct evidence of an electrochemical mechanism for the oxidation of water, since it is expected from this model that the transfer of positive charge $Ru(bpy)_3^{3+}$ to the ruthenium(IV) oxide particle and the release of a proton from water would be simultaneous events. However, it appears that in these experiments the workers involved did not actually monitor the evolution of oxygen either as a function of time or at the end of reaction and this may be a significant omission (*vide inra*). The kinetics were fitted to a first order decay for $Ru(bpy)_3^{3+}$ and were near to diffusion-contolled. However, the effect of pH and catalyst concentration on the first-order rate constant were found not to be simple or easily rationalized.

Harriman and his co-workers[23] have employed both colloidal hydrated ruthenium(IV) oxide (prepared chemically and using gamma radiolysis) and manganese(IV) oxide (prepared using gamma radiolysis) as $O_2$ catalysts. In testing these catalysts, both photochemically generated $Ru(bpy)_3^{3+}$ and $Ce^{IV}$ ions were used as the oxidant. Colloidal $MnO_2$ appeared to be a poor $O_2$ catalyst. They found that the hydrated ruthenium(IV) oxide colloids could catalyse the oxidation of water by $Ru(bpy)_3^{3+}$ or $Ce^{IV}$ ions. However, with both oxidants, corrosion was observed and appeared particularly serious (% corrosion = 23.4—40.2%) when $Ce^{IV}$ ions were used. The kinetics of $Ce^{IV}$ reduction (*via* $O_2$ catalysis, reaction 8, and corrosion, reaction 7) were briefly examined and the first-order rate constant appeared to depend directly upon the catalyst concentration.

Minero and his co-workers[22] have used a colloid of hydrated ruthenium(IV) oxide protected by polybrene and a colloid of $TiO_2$/hydrated ruthenium(IV) oxide as $O_2$ catalysts in the oxidation of water by $Ce^{IV}$ and $Ru(bpy)_3^{3+}$ ions. The colloid of $TiO_2$/hydrated ruthenium(IV) oxide is very similar to that used by Grätzel *et al.* in his flash conductiometric study. As in the latter kinetic study, Minero *et al.* used $Ru(bpy)_3^{3+}$ as the oxidant and found its decay to be first-order

over three half-lives. Not surprisingly, the observed variation of the first-order rate constant ($k_m$) with pH and catalyst concentration was similar to that reported by Grätzel and his co-workers.[39] Interestingly, the variation of $k_m$ with pH is very similar with and without the catalyst although the rate of the former reaction appears to be several hundred times greater.

It is appropriate at this point to identify a clear but often unstated danger associated with the interpretation of results arising from kinetic studies of reactions mediated by colloidal catalysts. Examples of such reactions will include: the oxidation of water to $O_2$, the oxidation of brine to $Cl_2$ by strong oxidants such as $Ce^{IV}$ or $Ru(bpy)_3^{3+}$ ions, and the reduction of water to hydrogen by strong reducing agents such as reduced methyl viologen. Clearly any mechanistic interpretation of the results following a kinetic study of such reactions may be badly flawed if it has not been proved that the appropriate gas is liberated in stoicheiometric proportions concomitant with the reduction of the oxidant, or oxidation of the reductant. Unfortunately, due to the limited response time of most gas analysis systems, it is often impossible to monitor the evolution of gas on the same time-scale as the colloidal kinetics. Under such circumstances the best that can be achieved is usually to ensure that gas evolution is quantitative under the conditions used in the kinetic study.

This problem with colloid kinetics has been well illustrated by the work of Albery and his co-workers in their investigation of the reduction of water by $MV^{+\bullet}$. They have had to modify their initial mechanistic interpretation[66] of the kinetics of $MV^{+\bullet}$ oxidation upon discovering that a significant contribution to the decay of the $MV^{+\bullet}$ was provided by the reduction of oxide on the surface of their Pt colloidal catalysts rather than water reduction.[67] In the case of water oxidation, before any mechanistic interpretation can be made of the results of a kinetic study of $O_2$ catalysis the question must be asked: are the observed kinetics solely due to water oxidation, rather than the oxidation of (i) a trace impurity in the solvent, (ii) a species other than water associated with the colloid (*e.g.* the supporting agent, or the catalyst itself) and/or (iii) the oxidant. Although the latter suggestion (iii) will not apply to $Ce^{IV}$ ions, it is well known that $Ru(bpy)_3^{3+}$ ions are unstable at all pHs, and susceptible to, amongst other things,[54,55] a 'deep disintegration' reaction[26,30] involving only a bpy ligand, *i.e.*

$$C_{10}H_8N_2(bpy) + 20H_2O - 48e^- \longrightarrow 10CO_2 + N_2 + 48H^+ \qquad (33)$$

This reaction appears to be efficient at both high and low pHs. From equation 33 the complete deep disintegration of only 1 molecule of $Ru(bpy)_3^{3+}$ would require 150 molecules of $Ru(bpy)_3^{3+}$. Unfortunately, when using $Ru(bpy)_3^{3+}$ as the oxidant, conductance measurements may not clearly identify water oxidation since protons are also liberated by this well established 'deep disintegration' reaction.[33]

In a kinetic study Minero and his group[22] used a colloid of hydrated ruthenium(IV) oxide supported by polybrene to mediate reaction 8 under

[67] W. J. Albery, P. N. Bartlett, and A. J. McMahon, *J. Electroanal. Chem.*, 1985, **182**, 7.

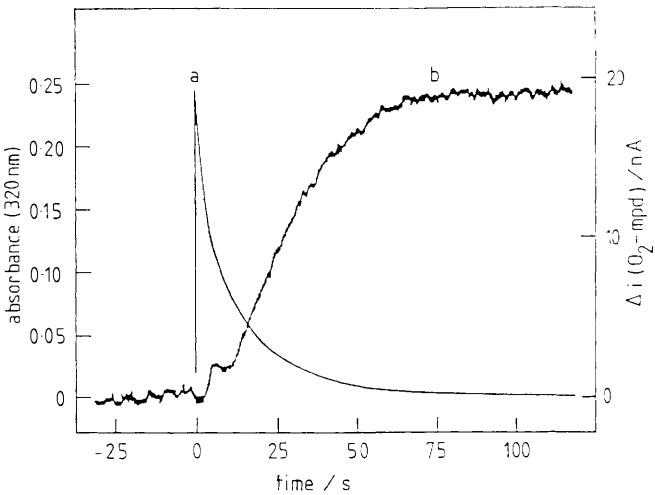


**Figure 14** *Oxidation of water to* $O_2$ *by* $Ce^{IV}$ *ions* ($4.5 \times 10^{-5}$) *in* 0.1 mol $dm^{-3}$ $H_2SO_4$, *mediated by a colloid of hydrated ruthenium*(IV) *oxide* (0.001 25 g $dm^{-3}$), *supported by polybrene* (0.000 63 g $dm^{-3}$). *The decay of the* $Ce^{IV}$ *ions* (*curve a*) *was monitored spectrophotometrically using a stopped-flow technique. The concomitant evolution of* $O_2$ (*curve b*) *was monitored polarographically using an* $O_2$-MPD. *The maximum change in current* [$\Delta i(O_2$-MPD)] *observed corresponded to a* 20% $O_2$ *yield*

conditions in which they believed 'dioxygen evolution should be the predominant pathway', *i.e.* $[Ce^{4+}] = 2—5 \times 10^{-5}$ mol $dm^{-3}$, [catalyst] = 0.0005—0.02 g $dm^{-3}$, polybrene 0.015 g $dm^{-3}$, and $H_2SO_4$ 0.09 mol $dm^{-3}$ at 25 °C. The decay of the $Ce^{IV}$ ions was found to be first order and $k_m$ was found to be directly dependent upon [catalyst]. We have since repeated this work[21] and confirmed the kinetic observations. However, using an oxygen membrane polarographic detector ($O_2$-MPD) to monitor any dissolved $O_2$ generated under the same conditions as the kinetic study we were *unable* to observe *any* $O_2$. We believe, therefore, that the kinetics reported by Minero *et al.*[22] and repeated by ourselves were not associated with the oxidation of water, but, rather the oxidation of the polybrene. In support of this latter suggestion, when the polybrene concentration was dropped from the constant value of 0.015 g $dm^{-3}$, independent of the colloid concentration, to a value which was always approximately half the catalyst concentration, % $O_2$ yields of 20% were observed as illustrated in Figure 14. On scaling up by a factor of 70 the system used to generate the results in Figure 14, in order to determine the % corrosion, it was found that the % corrosion was only 27% and the % $O_2$ yield had increased to 73%! As yet the reasons for the change in % yield remain unclear and a cause for concern.

*Acknowledgements.* I thank the SERC and Royal Society for supporting this work and all my fellow collaborators for their invaluable help and advice.